1967

Inelastic Behavior of Steel I-beams with Hexagonal Web Cutouts

Teresa Chen Wang

INELASTIC BEHAVIOR OF STEEL I-BEAMS WITH HEXAGONAL WEB CUTOUTS

BY

TERESA CHEN WANG

A thesis submitted
in partial fulfillment of the requirements for the
degree Master of Science, Major in Civil
Engineering, South Dakota
State University

1967

INELASTIC BEHAVIOR OF STEEL I-BEAMS

WITH HEXAGONAL WEB CUTOUTS

This thesis is approved as a creditable and independent investigation by a candidate for the degree, Master of Science, and is acceptable as meeting the thesis requirements for this degree, but without implying that the conclusions reached by the candidate are necessarily the conclusions of the major department.

Thesis Adviser Date

Head, Civil Engineering Department Date

ACKNOWLEDGMENT

The author wishes to express her sincere appreciation to Dr. Zaher Shoukry, Associate Professor, Department of Civil Engineering, for his criticism and guidance throughout the course of this project.

This thesis is dedicated to the author's mother, Pao whose continued encouragement and devotion has made this undertaking possible.

TCW

TABLE OF CONTENTS

LIST OF FIGURES

Figure Page

LIST OF TABLES

CHAPTER I

INTRODUCTION

General

In recent years plastic analysis has been widely used in structural design throughout the United States. It is based on the maximum load-carrying capacity of the structure. It offers a more realistic design approach than the conventional elastic methods, where the true factor of safety against ultimate strength can and does vary significantly from one structure to another.

The main objective of this study is to determine the maximum load-carrying capacity of steel I-beams with hexagonal web cutouts. When the cutouts are arranged as shown in Figure 1-a, the beam presents an appearance exactly as does a castellated beam.

A word relative to castellated beams may be appropriate here, however. A castellated beam consists of two halves of rolled-steel shapes joined by welding after the web has been cut in a zig zag line, thus producing a beam with increased depth and hexagonal holes in the web as shown in Figure 1-b. The load carrying-capacity and stiffness of this beam then become greater than the original un-expanded shape. The reduction in beam weight has a chain effect on savings throughout the structure. The analyses and conclusions in this study are applicable to castellated beams.

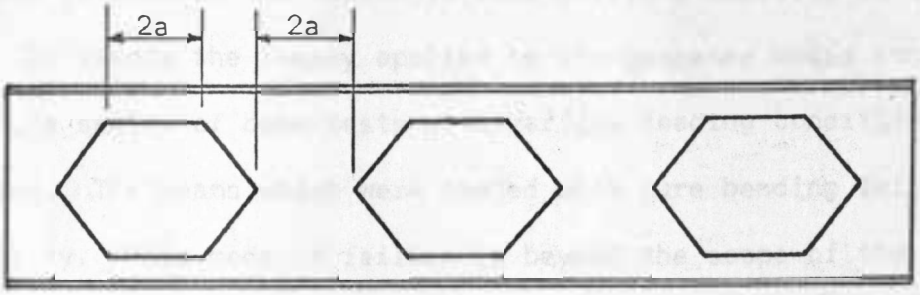

Beam with Hexagonal Cutouts

(a)

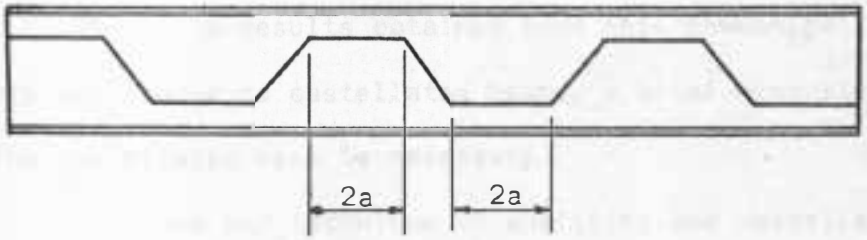

Web Cutting Pattern

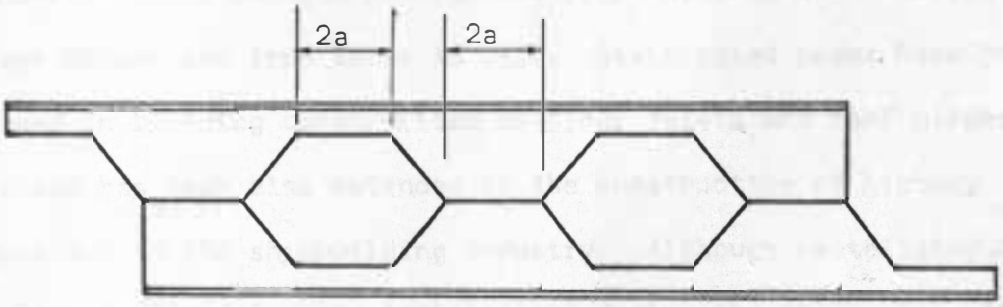

Expanded Shape

(b)

Figure 1. Castellated Beam

The Upper Bound Theorem[1] and the mechanism method of analysis were used to predict the inelastic load-carrying capacity of the beams. To insure the theory applied to the geometry under consideration, a series of beam tests with various loading conditions were conducted. The beams which were tested with pure bending failed by instability. This mode of failure is beyond the scope of the inelastic or fully-plastic analysis, which assumes the development of ideal, fully plastic hinges. However, when the beams were subjected to center loading, good agreement was noted between computed and measured failure loads.

Review of Previous Applications and Research

Since the results obtained from this investigation are mainly applicable to castellated beams, a brief historical review of the castellated beam is necessary.

The idea and technique of splitting and castellating beams to increase their section modulus was first used by H. E. Horton of Chicago Bridge and Iron Works in 1910. Castellated beams have been employed in building construction as floor joists and roof girders. Their use has been also extended to the construction of highway bridges and in the shipbuilding industry. Although castellated beams have been employed in many applications during the past years, their use is still limited. This is probably due to the following reasons:

---

[1] See Appendix 1.

1. The uncertainty of the load-carrying capacity of the beam because of the lack of an adequate design procedure.
2. An effective production process adaptable to mass production has not been developed.

In 1957, Altfillisch, Cooke and Toprac tested three expanded beams and studied their structual behavior both in the elastic and plastic range.[2] An approximate method of stress and deflection analysis was introduced.

Many reports are available which discuss the elastic behavior of various structural forms containing access holes of different shapes. In 1958, W. J. Worley reported his investigation of the effects of various elliptical web cutouts on the elastic and inelastic load-carrying capacity of aluminum alloy I-beams.[3] It was found that a diamond-shape cutout would yield the greatest load-carrying capacity per pound of beam weight. In his study, however, hexagonal web cutouts were not considered.

---

[2]M. D. Altfillisch, B. R. Cooke and A. A. Toprac, "An Investigation of Welded Open-Web Expanded Beams," Welding Research, (Supplement to the Welding Journal), Vol. 22, No. 2, February 1957, pp. 77s-88s.

[3]W. J. Worley, "Inelastic Behavior of Aluminum Alloy I-Beams with Web Cutouts," University of Illinois Engineering Experiment Station Bulletin No. 448, 1958.

Object and Scope of Investigation

The objectives of the investigation are as follows:

1. To investigate the effect of the hexagonal web cutouts on the load-carrying capacity of steel I-beams both in elastic and inelastic ranges.
2. To establish the most effective dimensions of the hexagonal web-cutout that would result in the least reduction in fully plastic load-carrying capacity of an I-beam.
3. To verify the Upper Bound Theorem procedure as an adequate method of predicting the fully-plastic load-carrying capacity for the beam with hexagonal web cutouts.
4. To compare the computer results with the test results.

The theoretical study was confined to I-beams which had one cutout on each end of the beam.

CHAPTER II

THEORETICAL ANALYSIS

Failure Theory

The main objective of this study was to determine the ultimate load-carrying capacity for steel I-beams with hexagonal cutouts. The ultimate load is usually obtained by using either the Mechanism Method or the Statical Method. The mechanism method has been adopted in this study for its simplicity and adaptability to computer programming.

According to the Upper Bound Theorem, the load computed on the basis of the assumed mechanism will always be greater or at best equal to the true ultimate load. If the problem is apprcached from that point by assuming a failure mechanism, an upper bound from which the correct load is obtained may perhaps violate the lower bound.[4] It is seen, therefore that the mechanism method represents an upper limit to the true ultimate load. To examine all possible collapse mechanisms, the work equation for each mechanism is written down and the corresponding value of the collapse load can be found. The actual collapse load will then be the smallest value thus obtained.

---

[4]L. S. Beedle, Plastic Design of Steel Frames, John Wiley & Sons, Inc., New York, 1958, p. 58.

A. Assumptions

In the subsequent analysis, the following assumptions are used:

1. Strains are proportional to the distance from the neutral axis.
2. The stress-strain relationship is idealized to consist of two straight lines as shown in Figure 2. The equations of these two lines are:

$$\sigma = E\epsilon \quad (0 < \epsilon < \epsilon_y) \qquad \text{elastic range}$$

$$\sigma = \sigma_y \quad (\epsilon_y < \epsilon < \infty) \qquad \text{plastic range}$$

where

σ = stress at distance y from neutral axis

σ_y = yield stress level

E = modulus of elasticity

ϵ = strain

ϵ_y = strain corresponding to theoretical onset of plastic yielding

The properties in compression are assumed to be the same as those in tension. Also, the behavior of fiber in bending is assumed to be the same as in tension or compression.

3. Instability of the structure will not occur prior to the attainment of the ultimate load.
4. The influences of normal and shearing forces on the plastic moment are neglected.
5. Stress concentrations which occur at abrupt changes in cross section are neglected.

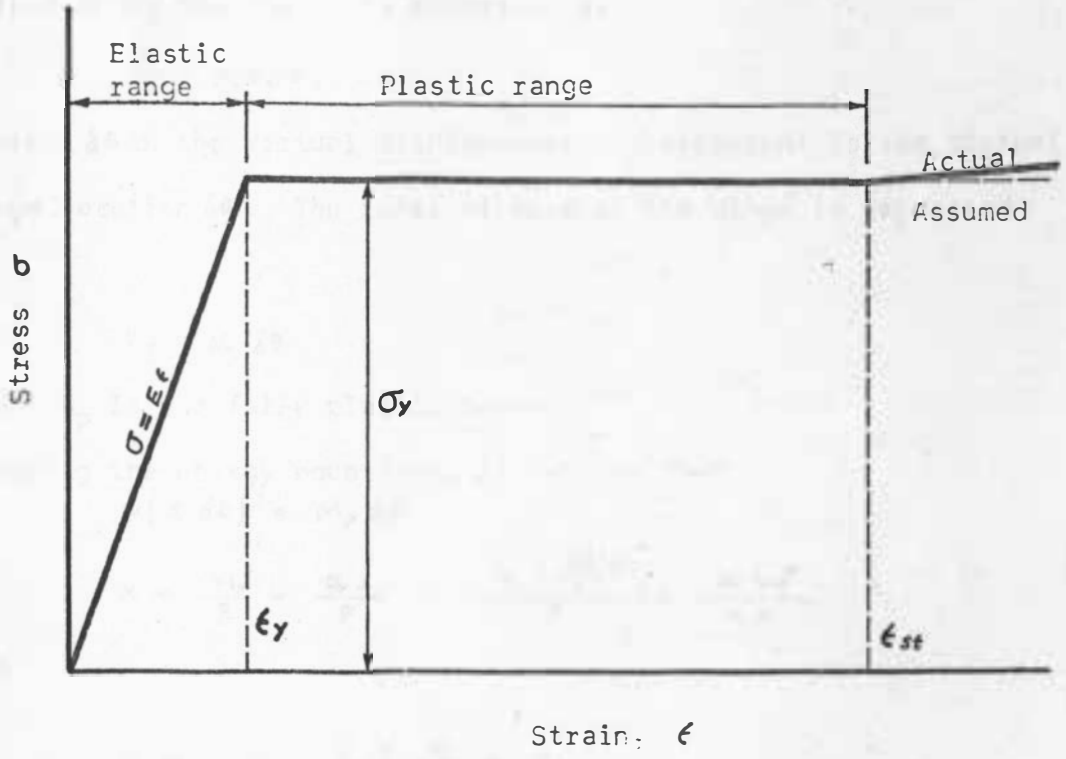

Figure 2. Idealized Stress-Strain Diagram

B. Analysis

A tapered cantilever beam with rectangular cross section is shown in Figure 3. It is assumed that the plastic hinge will form at a section distance x from the loading point A. The external work done by the load P is expressed as

$$W_E = P(x\,\delta\theta)$$

where $x\,\delta\theta$ is the virtual displacement correspondent to the virtual hinge rotation $\delta\theta$. The internal work at the hinge is expressed by

$$W_I = M_p\,\delta\theta$$

where M_p is the fully plastic moment.

Equating the energy equations, it follows that

$$P(x\,\delta\theta) = M_p\,\delta\theta$$

$$x = \frac{M_p}{P} = \frac{\sigma_y Z}{P} = \frac{\sigma_y \left(\frac{bd^2}{4}\right)}{P} = \frac{\sigma_y\, bd^2}{4P} \qquad (1)$$

and

$$d = (d_A - d_B)\frac{x}{\ell} + d_B$$

by substituting the value of d into equation (1), the hinge location can be found.

In case when the depth of the beam does not vary linearly, a function which gives the plastic modulus of the beam may also be found. The same method can be applied again to solve for the hinge location. The problem will be more complicated with the existence of any notch or hole in the section. In such case, a single hinge as

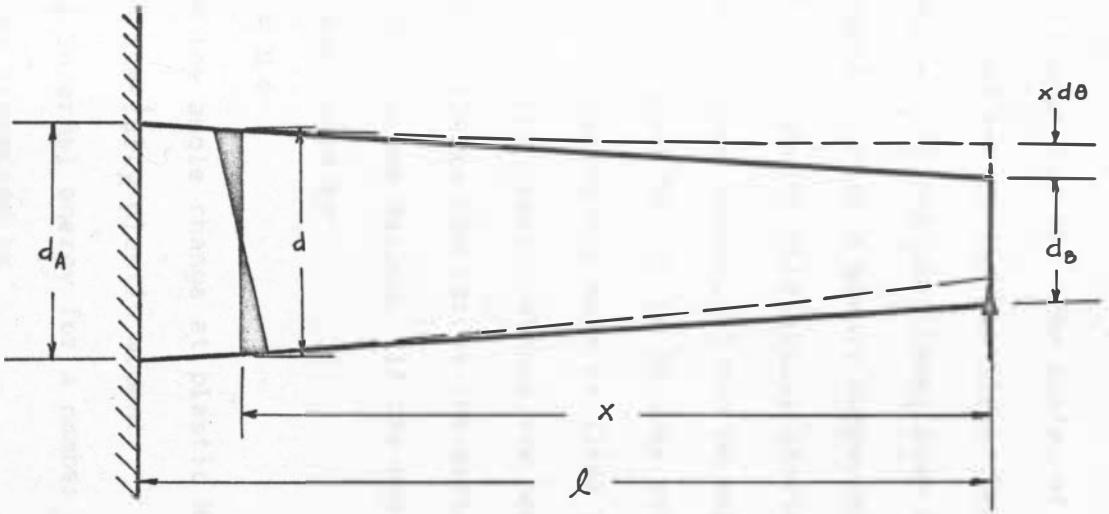

Figure 3. Plastic Hinge Formed in a Tapered Cantilever Beam

assumed above may not be enough to accomplish all the transfer of moment to carry out a failure mechanism. Therefore, further study has to be made.

The loading behavior of any simply supported beam with symmetrical loading can always be considered as a cantilever beam with a half span length. The center of the simply supported beam is then the fixed end of the cantilever beam. An upward load is applied at the free end of the cantilever beam as shown in Figure 4.

Figure 5 shows a simply supported steel I-beam with two hexagonal web cutouts bilaterally located symmetrical to the mid-span. In the same manner, it may be represented by a cantilever beam as shown in Figure 5. It is further assumed that the cutouts are big enough to become the most critical section of the beam.

Four fully plastic hinges are necessary to form a failure mechanism. This is similar to the action of a four bar linkage so familiar in machine design. If the energy required to form a plastic hinge is expressed by

$$U = M\Phi$$

where Φ = the angle change at plastic hinge

M = the fully plastic moment

The total internal energy for a number of fully plastic hinges, i, can then be expressed by

$$U = M_i\Phi_i$$

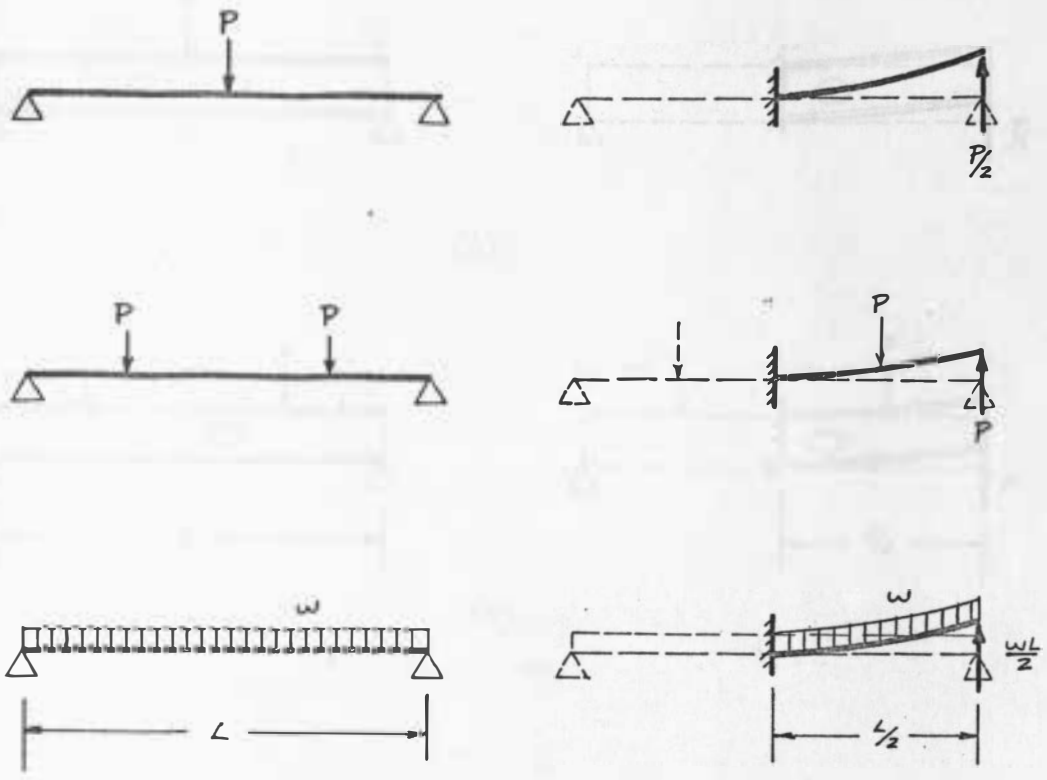

Figure 4. Correlation Between Simply Supported Beam and Cantilever Beam with Symmetrical Loading

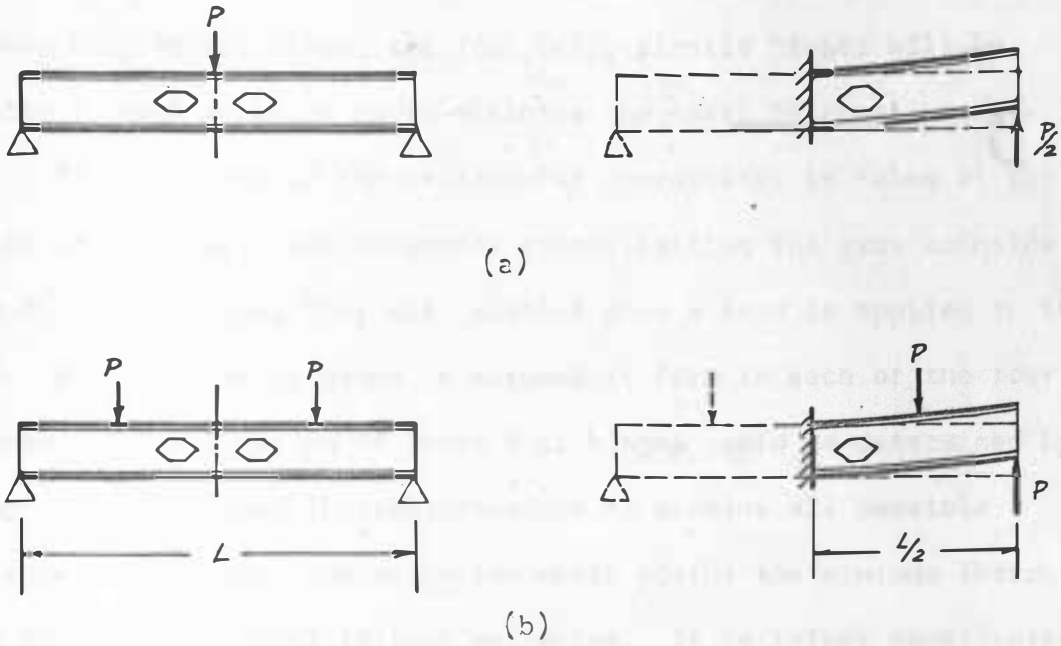

Figure 5. Correlation Between Simply Supported Beam and Cantilever Beam with Hexagonal Web Cutouts

By applying the theorem of least work[5], four hinges will then be the maximum requirement. The assumption of four fully plastic hinges is established.

The arrangement of these four fully plastic hinges is still unknown but, nevertheless, the four fully plastic hinges will be located in such a way so as to minimize the total internal energy.

If the origin of the rectangular coordinates is taken at the center of the undeformed hexagonal cutout letting the axes coincide with the cutout axes, they will distort when a load is applied to the beam. A fully plastic hinge is assumed to form in each of the four quadrants. The location of these four hinges could be determined by using the Upper Bound Theorem procedure to examine all possible collapse mechanisms. The mechanism which yields the minimum internal work done is the actual failure mechanism. It is rather complicated to carry out the necessary computations for all possible mechanisms, and therefore a digital electronic computer is employed to analyze the problem.

Mathematical Relations

A 6-inch steel junior beam was selected for study. The dimensions of the cross section of the beam, the shape of the cutout and the shape of the flange are shown in Figure 6. The cutout geometry can be expressed by two linear equations:

---

[5]F. R. Shanley, Strength of Materials, McGraw-Hill Book Company, Inc., New York, 1957, p. 30.

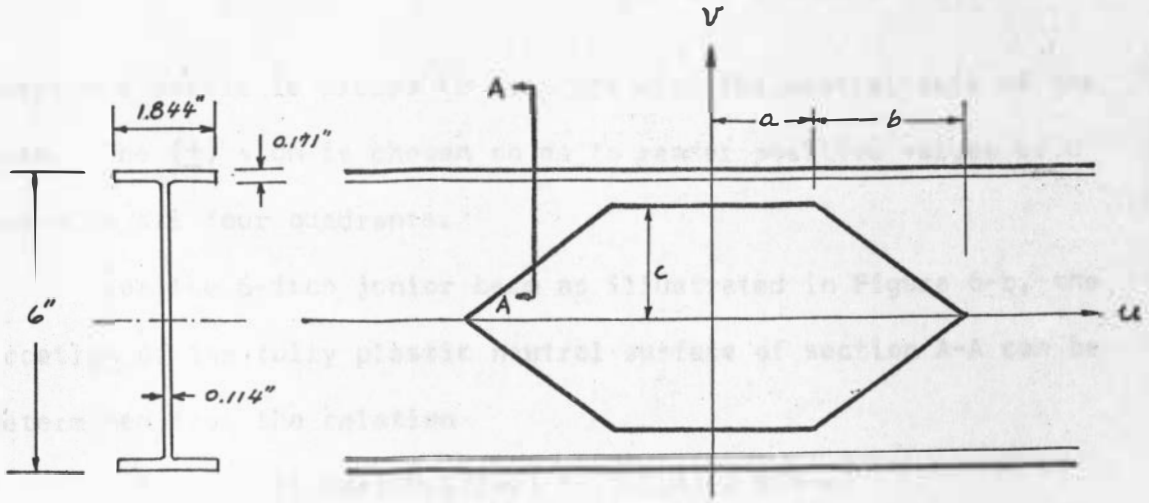

(a)

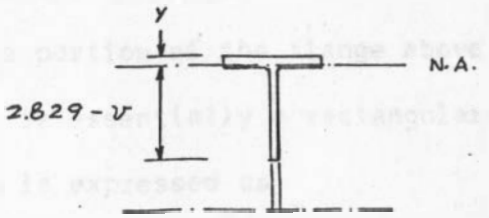

Section A-A

(b)

Figure 6. Dimensions and Cutout Geometry of the Beam

$$v = \pm c \qquad \text{for } u = 0 \text{ to } u = \pm a$$

$$v = \pm \frac{c}{b}\,(u - (a+b)) \qquad \text{for } u = \pm a \text{ to } u = \pm (a+b) \tag{2}$$

where the u-axis is placed to coincide with the neutral axis of the beam. The $(\pm)$ sign is chosen so as to render positive values of u and v in all four quadrants.

For the 6-inch junior beam as illustrated in Figure 6-b, the location of the fully plastic neutral surface of section A-A can be determined from the relation

$$1.844\ y = (1.844)(0.171-y) + (0.114)(2.829-v)$$

Hence

$$y = 0.17294 - 0.0309\ v \tag{3}$$

where y is the distance from the outer fiber of the flange to the fully plastic neutral surface.

Since the portion of the flange above the fully plastic neutral surface is essentially a rectangular section, the centroid of this portion is expressed as

$$\bar{y}_o = \tfrac{1}{2}\ y = 0.08647 - 0.01545\ v \tag{4}$$

The centroid of the portion of the web and flange below the fully plastic neutral surface was determined by

$$\Sigma(A\,Y) = (\Sigma A)\,\bar{y}$$

$$(0.114)(2.829-v)\left(\frac{2.829-v}{2} + (0.171-y)\right) + \tfrac{1}{2}(1.844)(0.171-y)^2$$
$$= \left[(0.114)(2.829-v) + (1.844)(0.171-y)\right]\bar{y}_i \qquad (5)$$

Substituting $y = 0.17294 - 0.0309\,v$ in equation (5) and solving for $\bar{y}_i$, it follows

$$\bar{y}_i = \frac{0.4559 - 0.3124\,v + 0.05436\,v^2}{0.3191 - 0.0570\,v} \qquad (6)$$

Figure 7 illustrates the failure mechanism, represented by four fully plastic hinges for each half of the simple beam.

From Figure 7,

$$L_1 = u_A + u_B \qquad (7)$$

$$L_3 = u_C + u_D \qquad (8)$$

$$L_2^2 = (u_B - u_C)^2 + (h - y_2 - y_3)^2 \qquad (9)$$

$$L_4^2 = (u_A - u_D)^2 + (h - y_1 - y_4)^2 \qquad (10)$$

also

$$\delta = \delta_o - \theta = \frac{\pi}{2} - \theta - \tan^{-1}\left[\frac{u_A - u_D}{\sqrt{L_4^2 - (u_A - u_D)^2}}\right] \qquad (11)$$

Equation (11), as well as equations (16), (17), and (18), which follow, were written in terms of $\tan^{-1}$ since the computer could not be programmed to solve $\sin^{-1}$ or $\cos^{-1}$ readily.

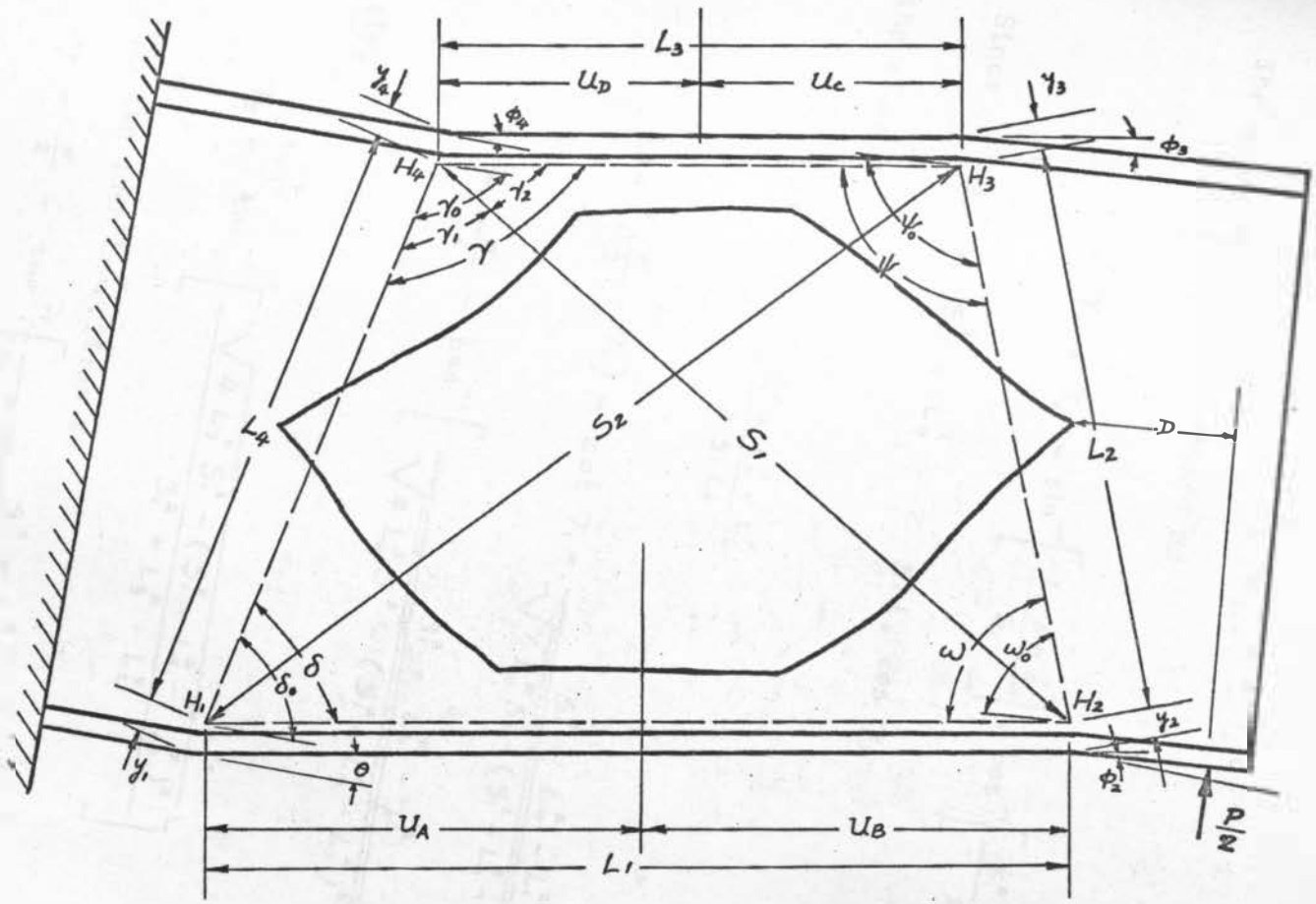

Figure 7. Beam Failure Mechanism

From Figure 7, the diagonal distance S_1 between the hinges H_2 and H_4 can be expressed in the form

$$S_1^2 = L_1^2 + L_4^2 - 2 L_1 L_4 \cos \delta \tag{12}$$

The angle γ can be expressed as

$$\gamma = \gamma_1 + \gamma_2 = \sin^{-1}\left[\frac{L_1 \sin \delta}{S_1}\right] + \cos^{-1}\left[\frac{S_1^2 + L_3^2 - L_2^2}{2 L_3 S_1}\right] \tag{13}$$

Since $L_1^2 = S_1^2 + L_4^2 - 2 S_1 L_4 \cos \gamma_1$

therefore

$$\cos \gamma_1 = \frac{S_1^2 + L_4^2 - L_1^2}{2 S_1 L_4}$$

$$\tan\left(\frac{\pi}{2} - \gamma_1\right) = \cot \gamma_1 = \frac{S_1^2 + L_4^2 - L_1^2}{\sqrt{4 L_4^2 S_1^2 - (S_1^2 + L_4^2 - L_1^2)^2}}$$

$$\gamma_1 = \frac{\pi}{2} - \tan^{-1}\left[\frac{S_1^2 + L_4^2 - L_1^2}{\sqrt{4 L_4^2 S_1^2 - (S_1^2 + L_4^2 - L_1^2)^2}}\right]$$

Similarly,

$$\gamma_2 = \tan^{-1}\left[\frac{\sqrt{4 L_3^2 S_1^2 - (S_1^2 + L_3^2 - L_2^2)^2}}{S_1^2 + L_3^2 - L_2^2}\right]$$

Equation (13) can then be written as

$$\gamma = \frac{\pi}{2} - \tan^{-1}\left[\frac{S_1^2 + L_4^2 - L_1^2}{\sqrt{4 S_1^2 L_4^2 - (S_1^2 + L_4^2 - L_1^2)^2}}\right] + \tan^{-1}\left[\frac{\sqrt{4 L_3^2 S_1^2 - (S_1^2 + L_3^2 - L_2^2)^2}}{S_1^2 + L_3^2 - L_2^2}\right] \tag{14}$$

The diagonal distance S_2 can be expressed as

$$S_2^2 = L_3^2 + L_4^2 - 2 L_3 L_4 \cos \gamma \tag{15}$$

Using the relations above, the angular displacement of the plastic hinges was computed with

$$\Phi_1 = \theta = 0.1 \text{ radian}$$

which is an arbitrary value approximating the actual measurements for the beams.

$$\Phi_2 = \omega - \omega_o = \left[\frac{\pi}{2} - \tan^{-1} \frac{L_1^2 + L_2^2 - S_2^2}{\sqrt{4 L_1^2 L_2^2 - (L_1^2 + L_2^2 - S_2^2)^2}}\right] - \left[\frac{\pi}{2} - \tan^{-1} \frac{u_B - u_C}{\sqrt{L_2^2 - (u_B - u_C)^2}}\right] \tag{16}$$

$$= \tan^{-1}\left[\frac{u_B - u_C}{\sqrt{L_2^2 - (u_B - u_C)^2}}\right] - \tan^{-1}\left[\frac{L_1^2 + L_2^2 - S_2^2}{\sqrt{4 L_1^2 L_2^2 - (L_1^2 + L_2^2 - S_2^2)^2}}\right]$$

$$\Phi_3 = \psi_o - \psi = \left[\frac{\pi}{2} + \tan^{-1} \frac{u_B - u_C}{\sqrt{L_2^2 - (u_B - u_C)^2}}\right] - \left[\frac{\pi}{2} - \tan^{-1} \frac{L_2^2 + L_3^2 - S_1^2}{\sqrt{4 L_2^2 L_3^2 - (L_2^2 + L_3^2 - S_1^2)^2}}\right] \tag{17}$$

$$= \tan^{-1}\left[\frac{L_2^2 + L_3^2 - S_1^2}{\sqrt{4 L_2^2 L_3^2 - (L_2^2 + L_3^2 - S_1^2)^2}}\right] + \tan^{-1}\left[\frac{u_B - u_C}{\sqrt{L_2^2 - (u_B - u_C)^2}}\right]$$

$$\Phi_4 = \gamma - \gamma_o \tag{18}$$

$$= \gamma - (\pi - \delta_o)$$

$$= \gamma + \delta_o - \pi$$

The area of the section where the plastic hinge occurs can be expressed by

$$A_t = (1.844)(0.171) + (2.829-c)(0.114) + (c - v)(0.114)$$
$$= 0.3813 - (0.114)(c - v)$$

When the internal work done by the four fully plastic hinges is equated to the external work done by the load, P/2, it follows

$$\frac{P}{2}\left[L_1\theta + (a + b + D - u_B)(\theta - \phi_2)\right] = \sigma_y \sum_{n=1}^{4}\left[\phi_n \frac{A_t}{2}(\bar{y}_o + \bar{y}_i)_n\right] \qquad (19)$$

or

$$P = \frac{\sigma_y \sum_{n=1}^{4}\left[\phi_n A_t (\bar{y}_o + \bar{y}_i)_n\right]}{L_1\theta + (a+b+D-u_B)(\theta-\phi_2)} \qquad (20)$$

where n denotes a particular hinge and σ_y is the yield stress of the beam. To determine the value of σ_y, three tension coupons were tested. The specimens were taken from the web section of the 6-inch junior beam. Test results are summarized in Table I and the average yield point was found to be 46,500 psi. However, an original value of 36,000 psi was assumed for the computer analysis. All computer results were then adjusted for a yield stress σ_y of 46,500 psi when comparing analytical and experimental results.

TABLE I

Static Tension Tests

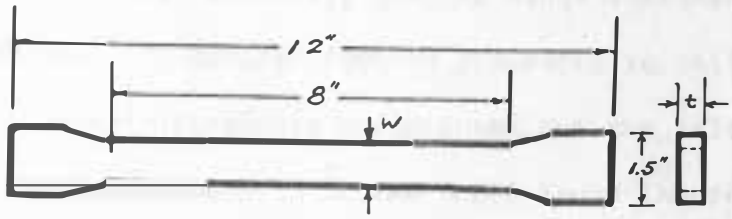

Specimen	Width w (inches)	Thickness t (inches)	Axial Load Corresponding to Yield Stress Level P_y (pounds)	$\sigma_y = \frac{P_y}{wt}$ (psi)
1	1.000	0.125	5,800	46,400
2	1.025	0.125	5,940	46,400
3	0.969	0.124	5,620	46,700

Average σ_y = 46,500 psi

Computer Programming and Results

In programming the problem for solution on the computer, the dimensions of the hexagonal cutout were given but the hinge locations were not known. Therefore, arbitrary initial hinge locations were fed into the machine. The program routine proceeded to shift the hinge locations in small increments and printed out the critical load for each location. According to the Upper Bound Theorem, the minimum load value will be the ultimate load. The corresponding mechanism gives the location of the four plastic hinges.

A general flow diagram is shown below to offer an easy notation for analyzing the steps required in the solution of the problem.

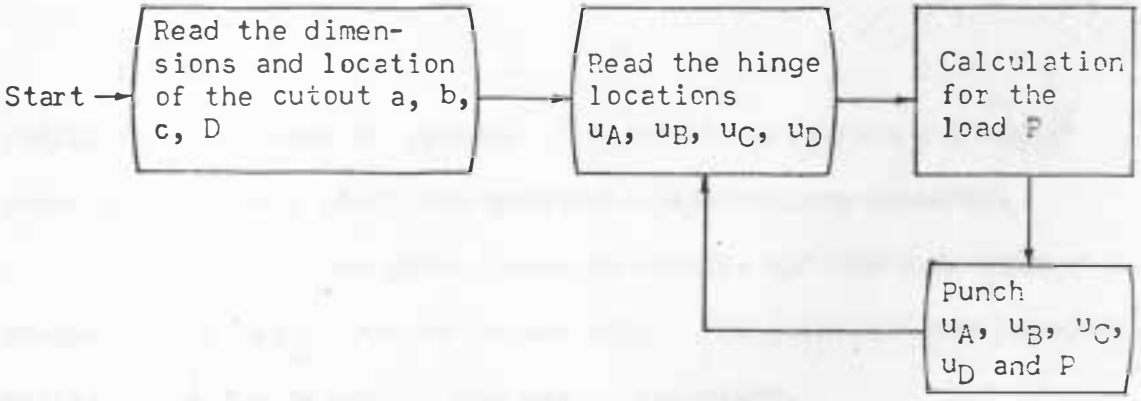

A computer program as shown in Appendix 2 was written accordingly. As it is impossible to consider every possible location for u_A, u_B, u_C, or u_D, therefore, a successive approximation method

was introduced. This method involves the determination of the critical load, P, using large location increments for the position of the plastic hinges. Finer increments were then introduced in the vicinity of the plastic hinges obtained before, giving a more accurate position and value for plastic hinges and ultimate load P_u. After approximating in this manner several times the required accuracy may be reached.

Table II shows computer results for a 6-inch junior beam with one hexagonal web cutout on either half of the beam and loaded at the midspan. The case where

$a = 0$

$b = 5$

indicates a diamond-shape cutout and where

$a = 5$

$b = 0$

indicates a rectangular cutout. The results predicted a diamond-shape cutout would yield the greatest load-carrying capacity.

Table III shows other computer results for the same beam with change in the height of the cutout only. The load-carrying capacity decreased as the height of the cutout increased.

From Tables II and III, curves were plotted and are shown in Figures 8 and 9 to illustrate the effects of height and shape of hexagonal web cutouts on the fully plastic load-carrying capacity of the beam.

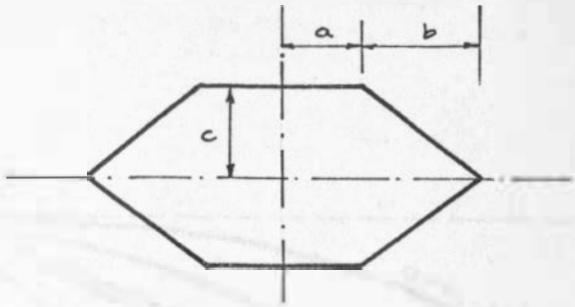

TABLE II

Computer Results for the Position of Plastic Hinges and Ultimate Load
(Depth of Cut = 4.5 inches)

a (inches)	b (inches)	c (inches)	u_A (inches)	u_B (inches)	u_C (inches)	u_D (inches)	P_u (pounds)
0	5	2.25	5.0	5.0	0.5	0.5	3,938
1	4	2.25	5.0	5.0	0.5	0.5	3,183
2	3	2.25	2.0	2.0	2.0	2.0	2,752
3	2	2.25	3.5	3.5	0.5	0.5	2,467
4	1	2.25	3.5	3.5	3.5	3.5	1,572
5	0	2.25	5.0	5.0	5.0	5.0	1,100

TABLE III

Computer Results for the Position of Plastic Hinges and Ultimate Load
(Depth of Cut = 5.5 inches)

a (inches)	b (inches)	c (inches)	u_A (inches)	u_B (inches)	u_C (inches)	u_D (inches)	P_u (pounds)
0	5	2.75	5.0	5.0	0.5	0.5	2,952
1	4	2.75	2.0	2.0	0.5	0.5	2,283
2	3	2.75	2.0	2.0	2.0	2.0	1,297
3	2	2.75	3.5	3.5	0.5	0.5	1,288
4	1	2.75	3.5	3.5	3.5	3.5	741
5	0	2.75	5.0	5.0	5.0	5.0	518

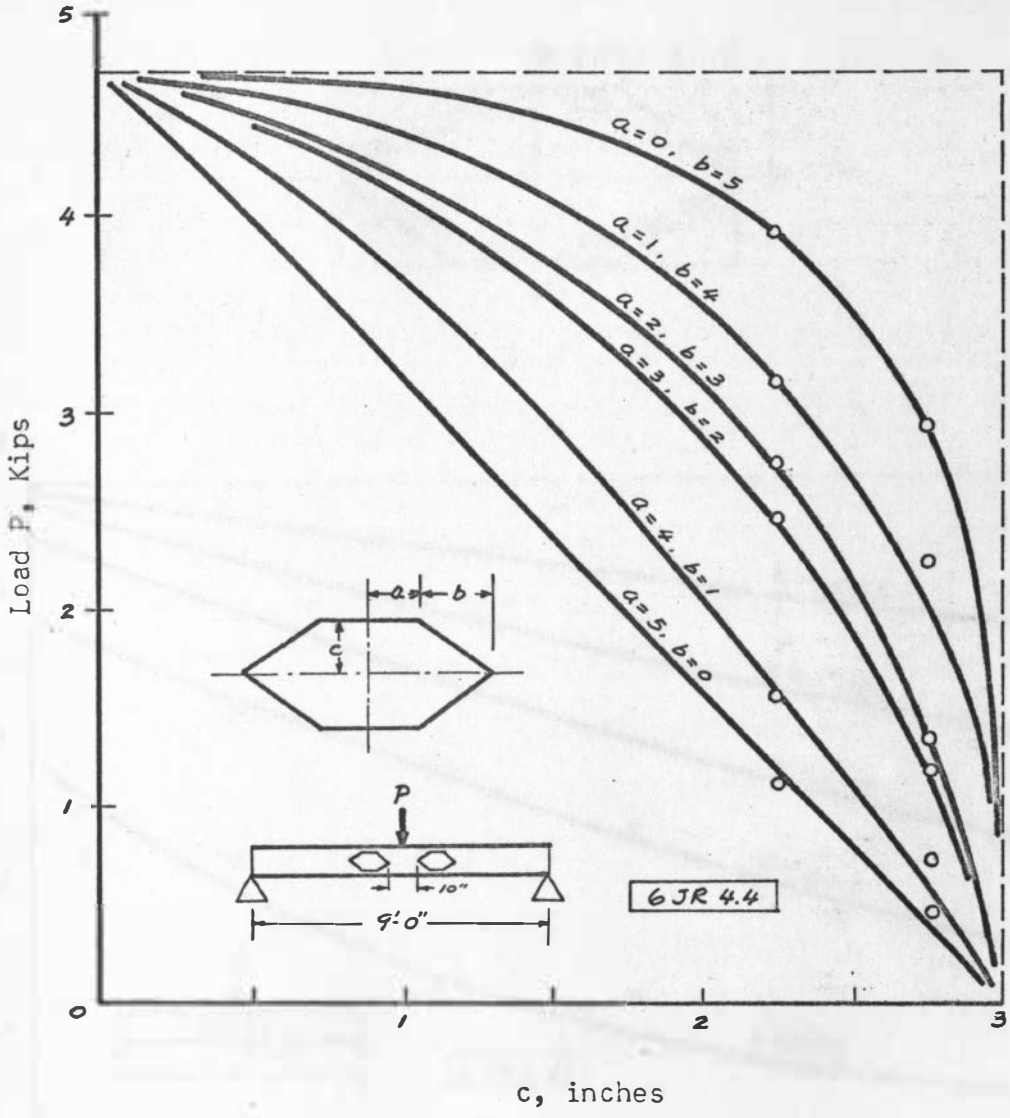

Figure 8. Effect of Height of Hexagonal Web Cutouts on Ultimate Load.

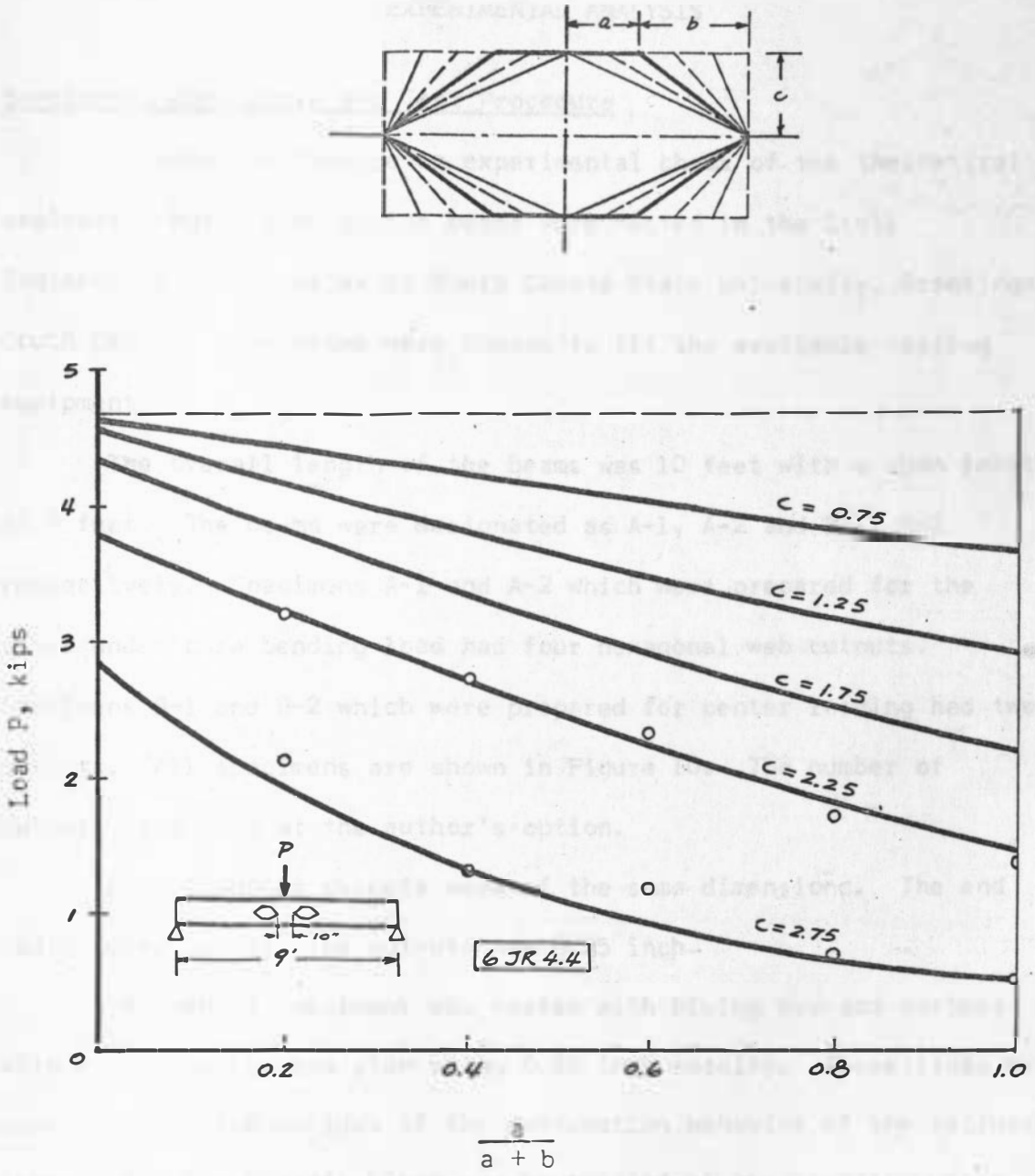

Figure 9. Effect of Shape of Hexagonal Web Cutouts on the Ultimate Load.

CHAPTER III

EXPERIMENTAL ANALYSIS

Specimens, Apparatus, and Test Procedure

In order to provide an experimental check of the theoretical analysis, four 6 inch junior beams were tested in the Civil Engineering Laboratories at South Dakota State University, Brookings, South Dakota. The beams were chosen to fit the available testing equipment.

The overall length of the beams was 10 feet with a span length of 9 feet. The beams were designated as A-1, A-2 and B-1, B-2 respectively. Specimens A-1 and A-2 which were prepared for the tests under pure bending load had four hexagonal web cutouts. Specimens B-1 and B-2 which were prepared for center loading had two cutouts. All specimens are shown in Figure 10. The number of cutouts were made at the author's option.

All hexagonal cutouts were of the same dimensions. The end radius used for all the cutouts was 0.25 inch.

The web of specimens was coated with bluing dye and scribed with grid lines on one side using 0.25 inch spacing. These lines were used to establish an idea of the deformation behavior of the failure mechanism. The plastic hinge may be located at the position where the lines bend abruptly. The opposite side of the web was painted with whitewash to detect the yielding zone and to locate the plastic hinges.

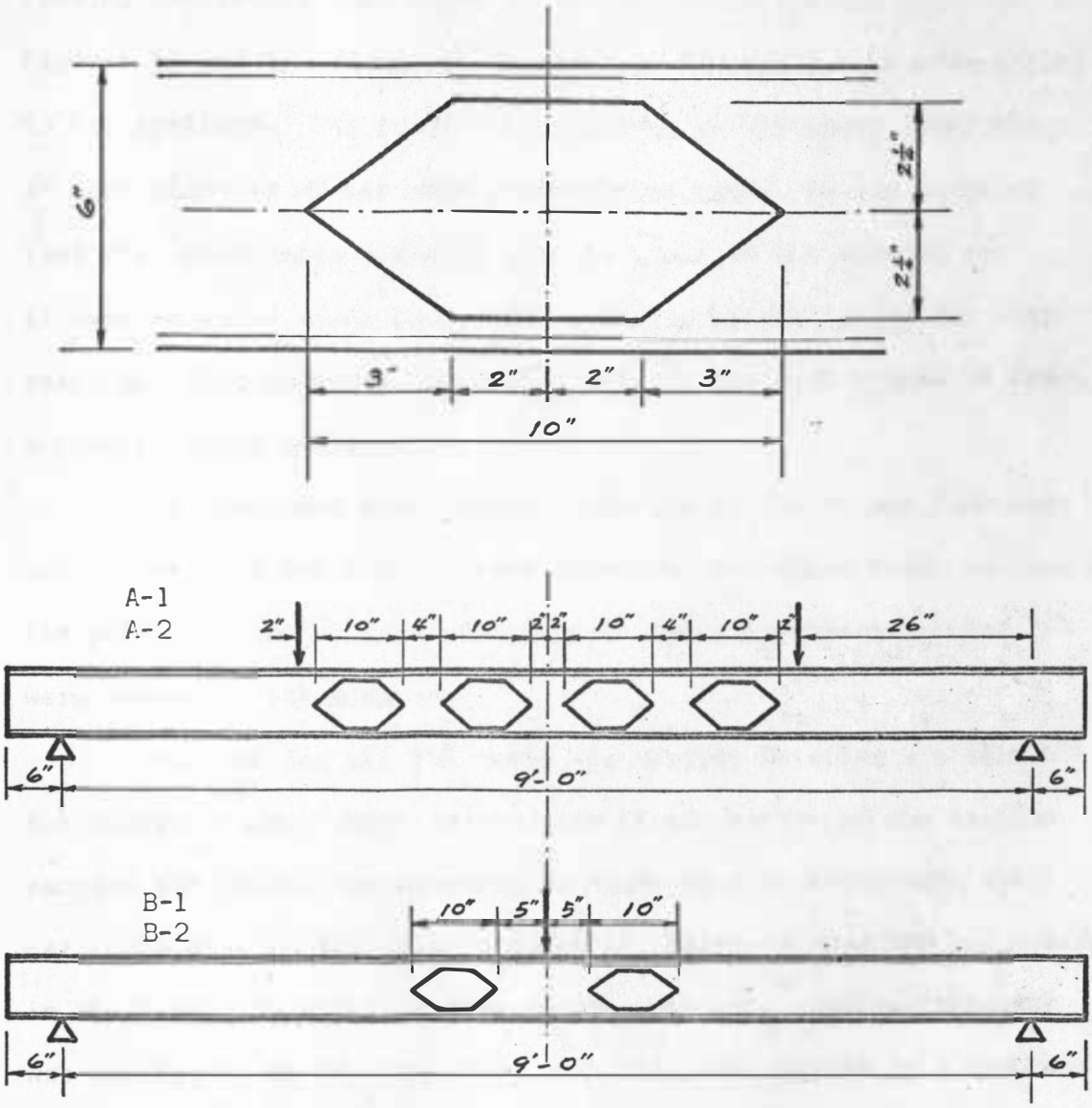

Figure 10. Dimensions of Test Specimens

A 15 foot loading frame was used for all beam tests. The loading apparatus, dial gages and lateral supports are shown in Figures 11 and 12. Load was transferred through a half-moon roller to the specimen. The loading was applied at 218 pound intervals, an equivalent to 20 psi gage reading each time. In the range of load when pronounced yielding occurred, one to two minutes was allowed to lapse after each loading period before taking the load reading. This interval was sufficient for the entire beam to reach a nearly stable state.

All specimens were simply supported at six inches from each end. Specimens A-1 and A-2 were loaded by two equal loads applied at the points 26 inches from each support while specimens B-1 and B-2 were loaded at the midspan.

The load for all the tests was applied by using a single 60-ton hydraulic jack which was located at the bottom of the testing machine and pulled the assembly by means of a high-strength steel bar. The dial on the console shown in Figure 13 read the psi pressure in the line. In order to interpolate the exact reading, the jack was calibrated by proving rings with the load applied by a compression testing machine. A jack factor of 10.9 was determined.

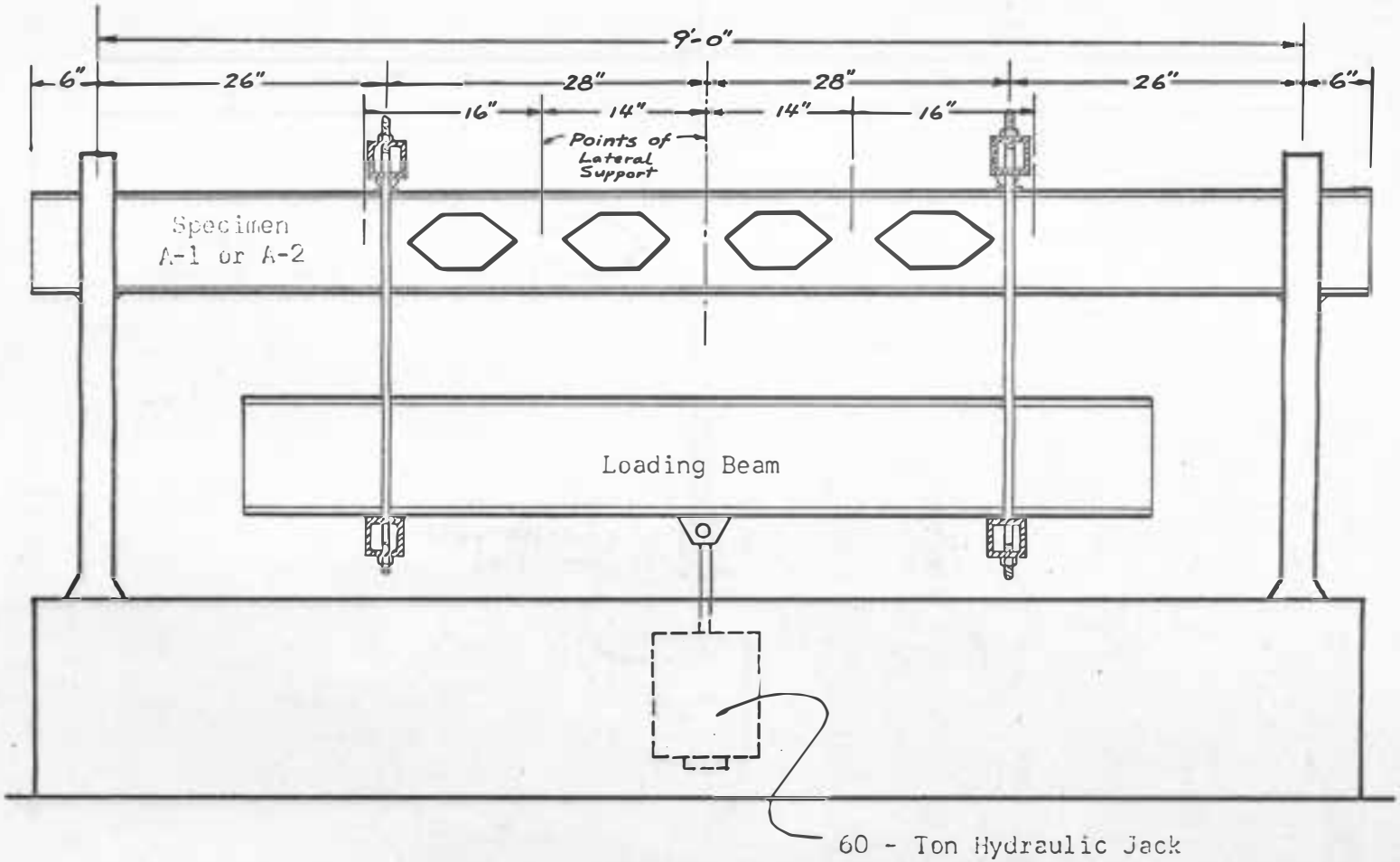

Figure 11. Pure Bending Apparatus

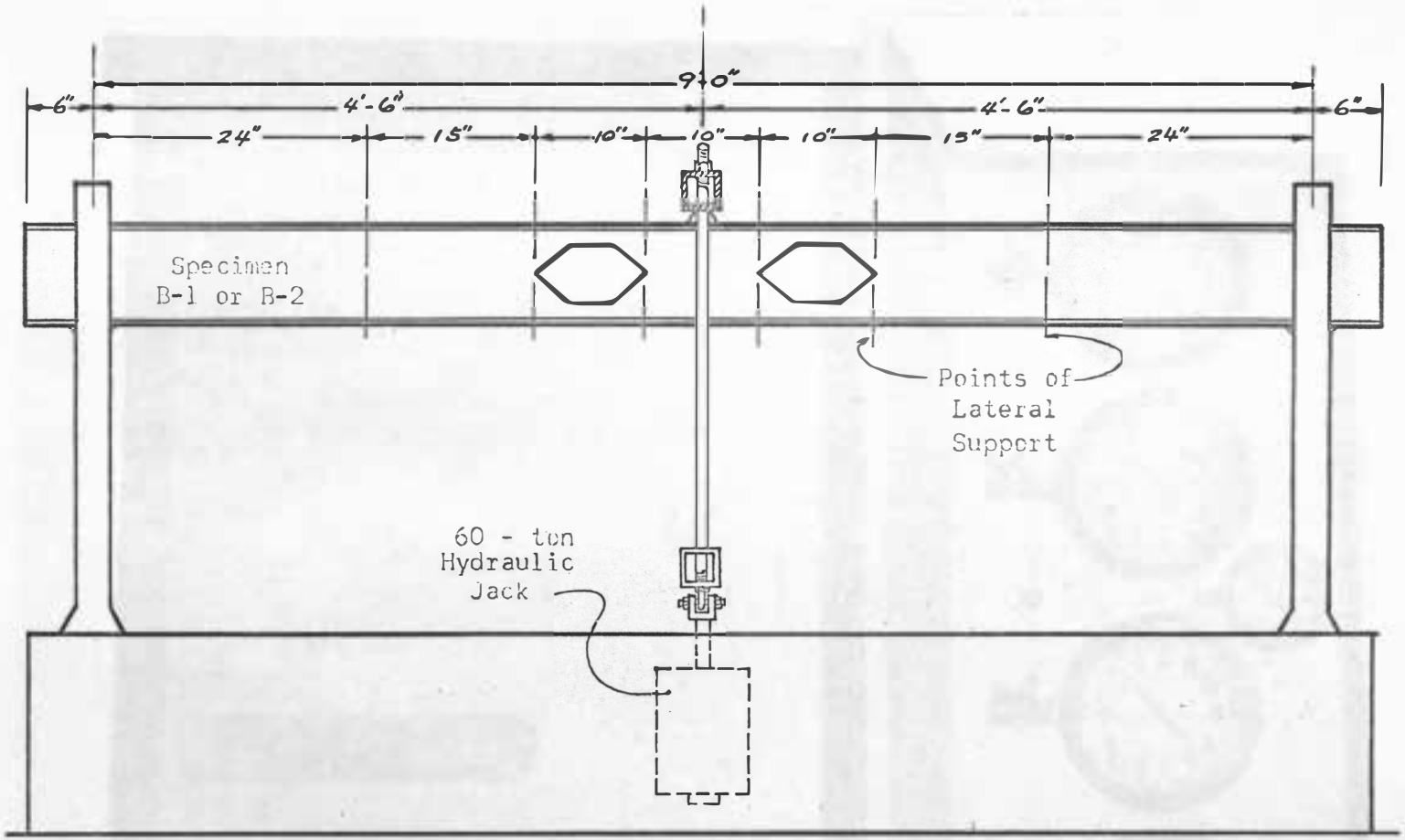

Figure 12. Center Loading Apparatus

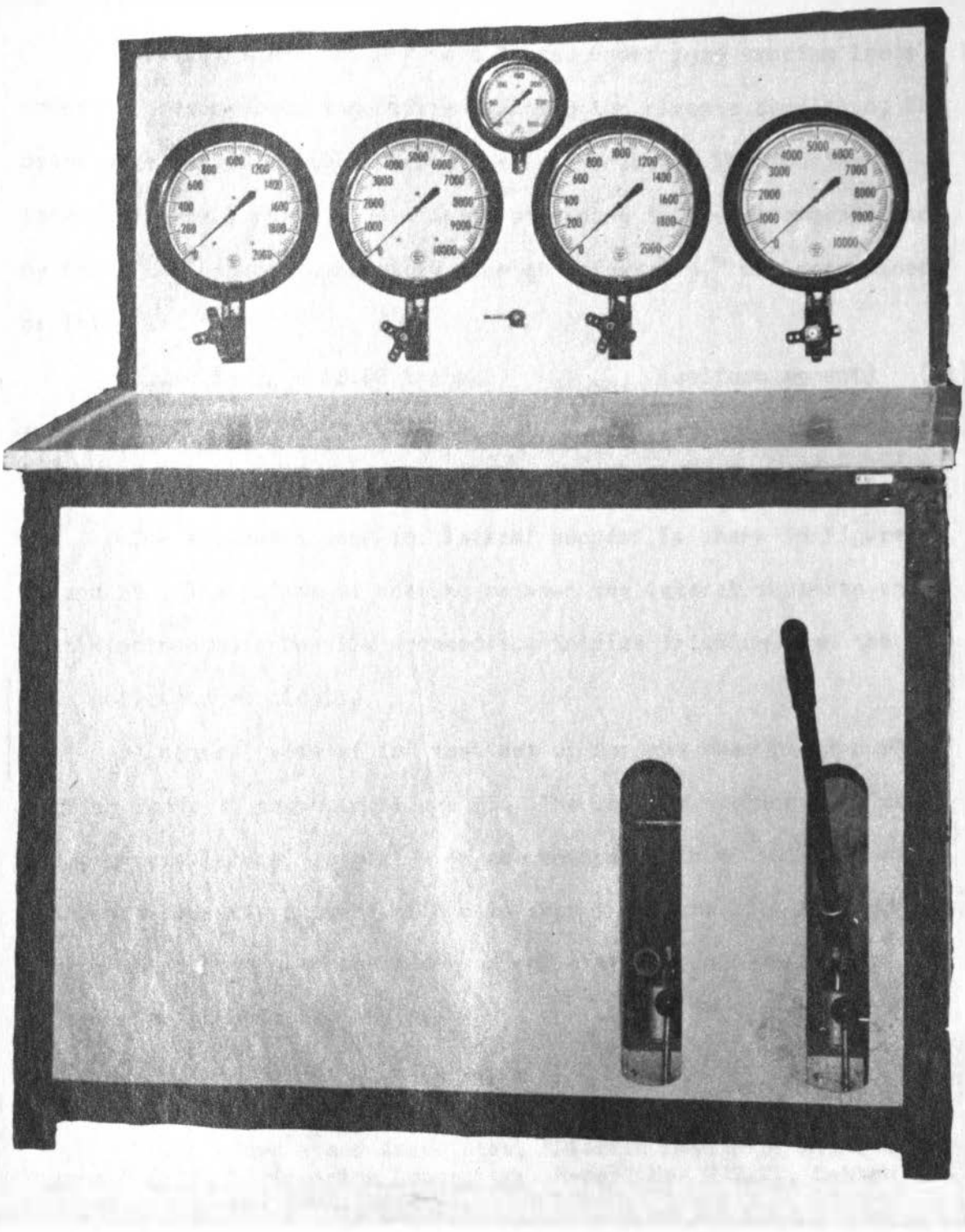

Figure 13. Dial Consol

Testing Program

A. Pure Bending

Specimens A-1 and A-2 were tested under pure bending loads. In order to prevent buckling before reaching the plastic condition, the beams were laterally supported at certain points. The spacing of lateral supports for a 6JR4.4 beam, according to the recommendation by Fritz Engineering Laboratory, Lehigh University,[6] was determined as follows:

$$L_{cr} = 38\ r_y = 13.68 \text{ inches} \qquad \text{(uniform moment)} \qquad (21)$$

and

$$L_{cr} = 65\ r_y = 23.40 \text{ inches} \qquad \text{(moment gradient)} \qquad (22)$$

where r_y is the radius of gyration with respect to the Y-Y axis.

The apparatus used for lateral support is shown in Figures 14 and 15. The points of bearing between the lateral supports and test specimen were heavily greased to minimize friction when the beam deflected vertically.

A general view of the test set up for the beam under pure bending loads is shown in Figure 11. The loading machine provided a clamp-type lateral support over the entire depth of the beam at both ends over the support as can be seen in Figure 15. Dial gages were mounted at the center and loading points to determine the deformation behavior of the beam.

---

[6] L. S. Beedle and Associates, "Plastic Design of Multi-Story Frames," Fritz Engineering Laboratory, Report No. 273.20, Lehigh University, Summer 1965, p. 3.21.

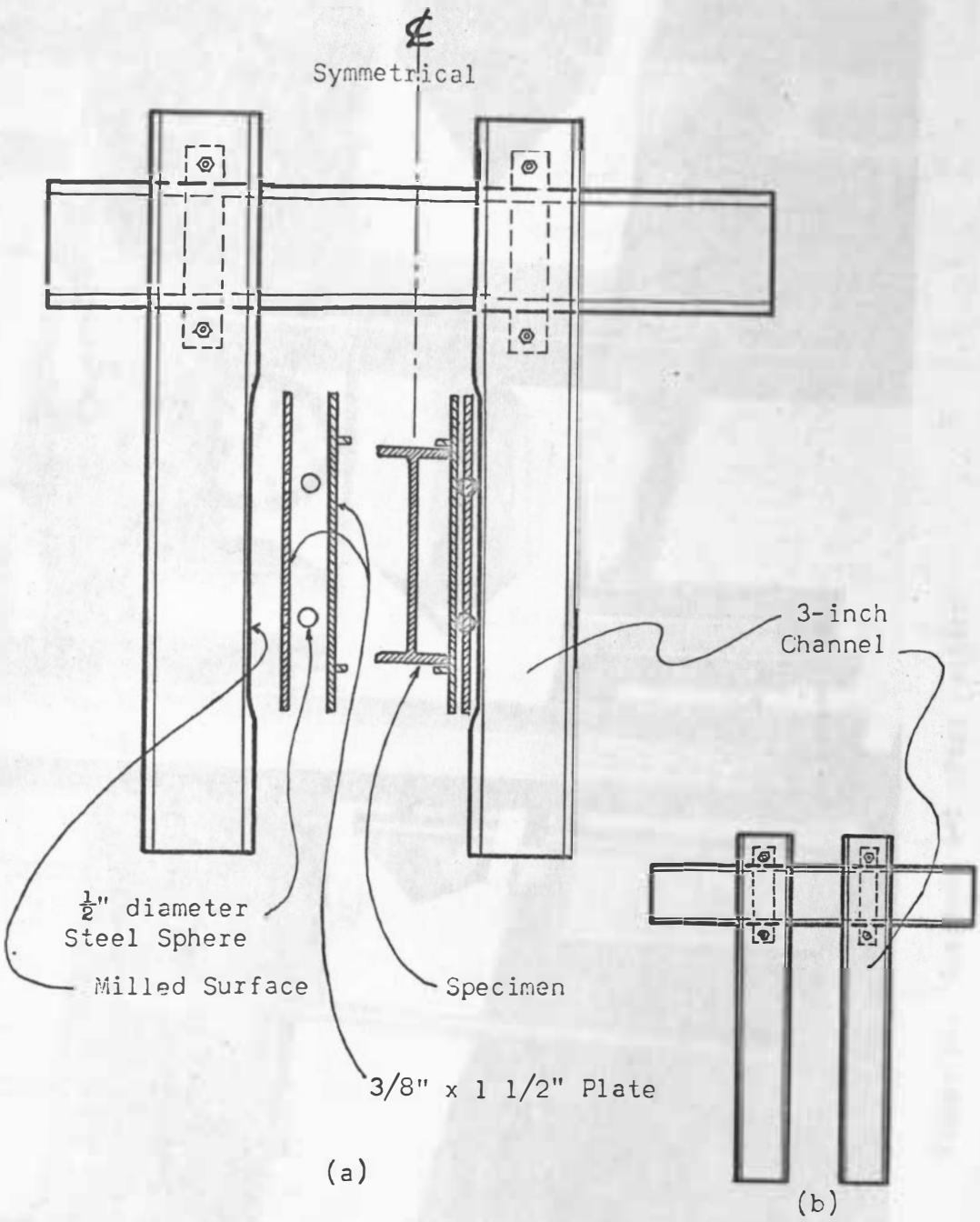

Figure 14. Details of Lateral Support

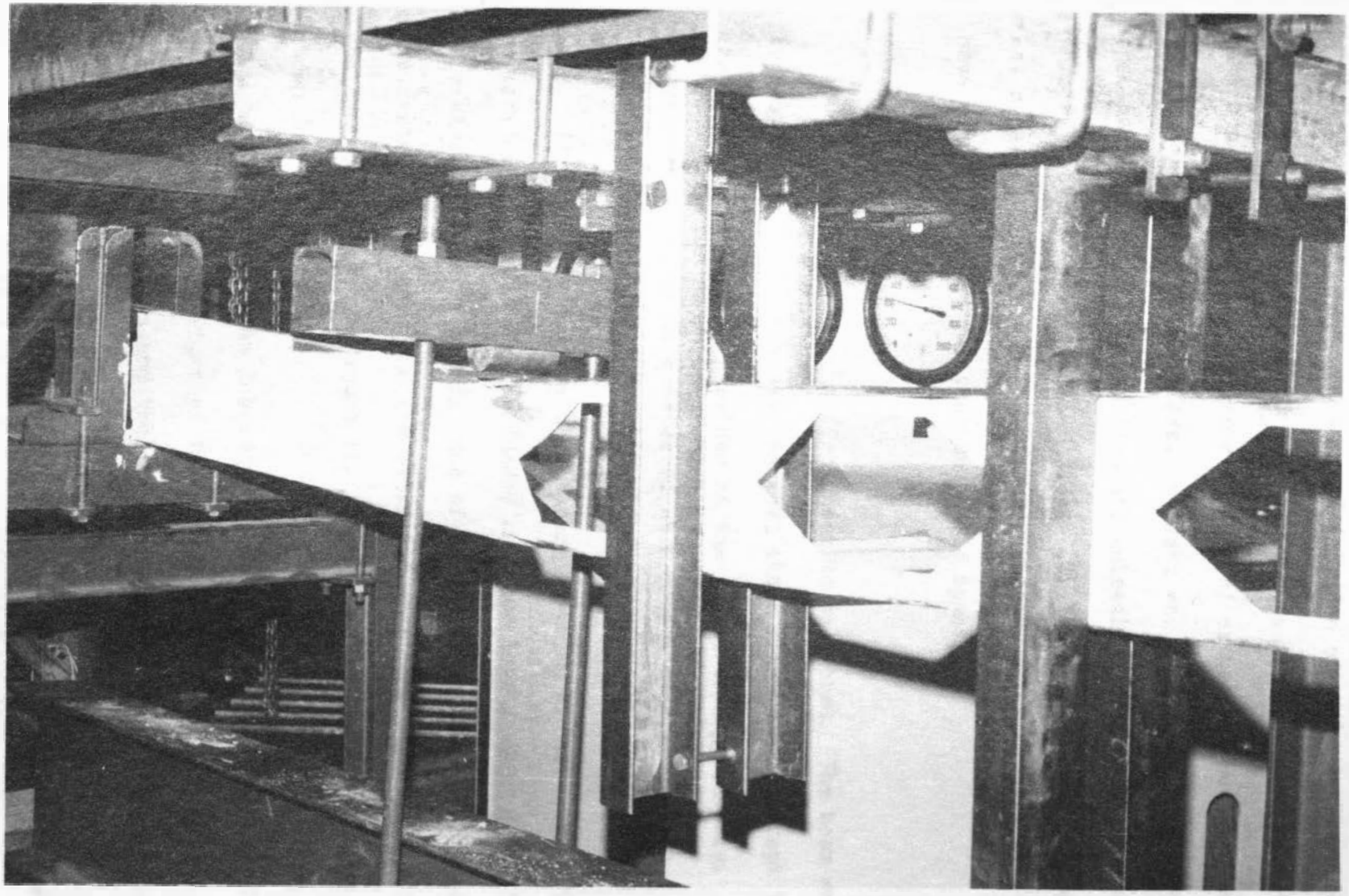

Figure 15. Specimen A-1 After Failure

As residual stresses cause initiation of yield at loads lower than that predicted by usual stress analysis and may also lower the ultimate capacity by inducing either local or general buckling of a compression element, therefore, the test was started by loading the specimen with a 1,500 pound load and unloading it without taking any readings of the deflection dials. This loading and unloading was repeated several times to release any residual stresses that may have resulted during fabrication of the beams.

Specimen A-1

Specimen A-1 was the first beam to be tested. The beam was loaded at two points the same as that shown in Figure 11 except that the lateral bracing was provided at the points of support only. Lateral deformations were detected at a moment of 2,770 ft-lbs which was much below the elastic load-carrying capacity of the beam. It was quite obvious that lateral bracing of the beam must be provided. The beam was unloaded and then loaded again after three lateral supports were added. One of the lateral supports was placed at the center of the beam and the other two were located 14 inches from the center as shown in Figure 11. The lateral support device is shown in Figure 14-b.

The beam was then loaded to a moment of 7,535 ft-lbs. This moment included the weight of the assembly hanging on the beam. The pump dial readings and the corresponding loads and moments for each beam are given in Appendix 3. Because of the weight of the assembly, the deflection curves do not start from zero load. The

load was applied at 218 pound intervals. At the end of every interval the loading was stopped and readings were recorded for the deflection dials. When a moment of 7,535 ft-lbs was reached, the final reading was taken and the beam failed by lateral buckling. As it can be seen from Figures 15 and 16, this failure was followed by the region under the upper left loading pad. A moment of 8,062 ft-lbs was recorded as the final reading. Figure 17 shows the relationship between load and deflection for the beam.

Specimen A-2

Before testing beam A-2, some modifications and revisions were made to the lateral support system. Two more lateral supports were placed at the points of loading. Two 3/8" x 1 1/2" steel plates and two steel spheres of 1/2 inch diameter were placed between the specimen and the lateral support. Figure 14-a shows the details of the lateral support arrangement. The diameter of these holes was 1/16 inch larger than that of the steel sphere so that the steel sphere might rotate freely. All contacted bearing surfaces were heavily greased.

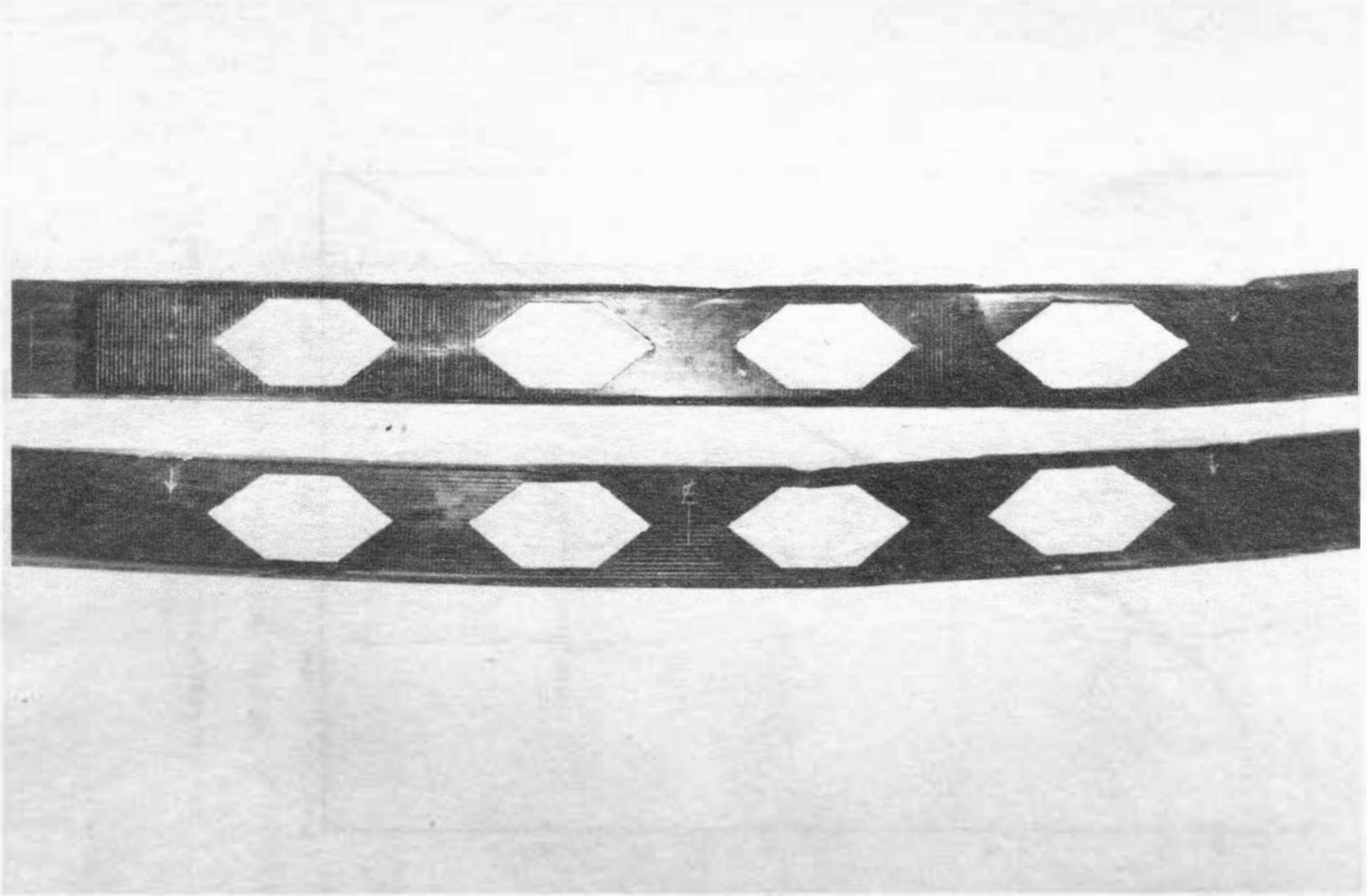

Figure 16. Front View of Specimens A-1 and A-2 After Testing

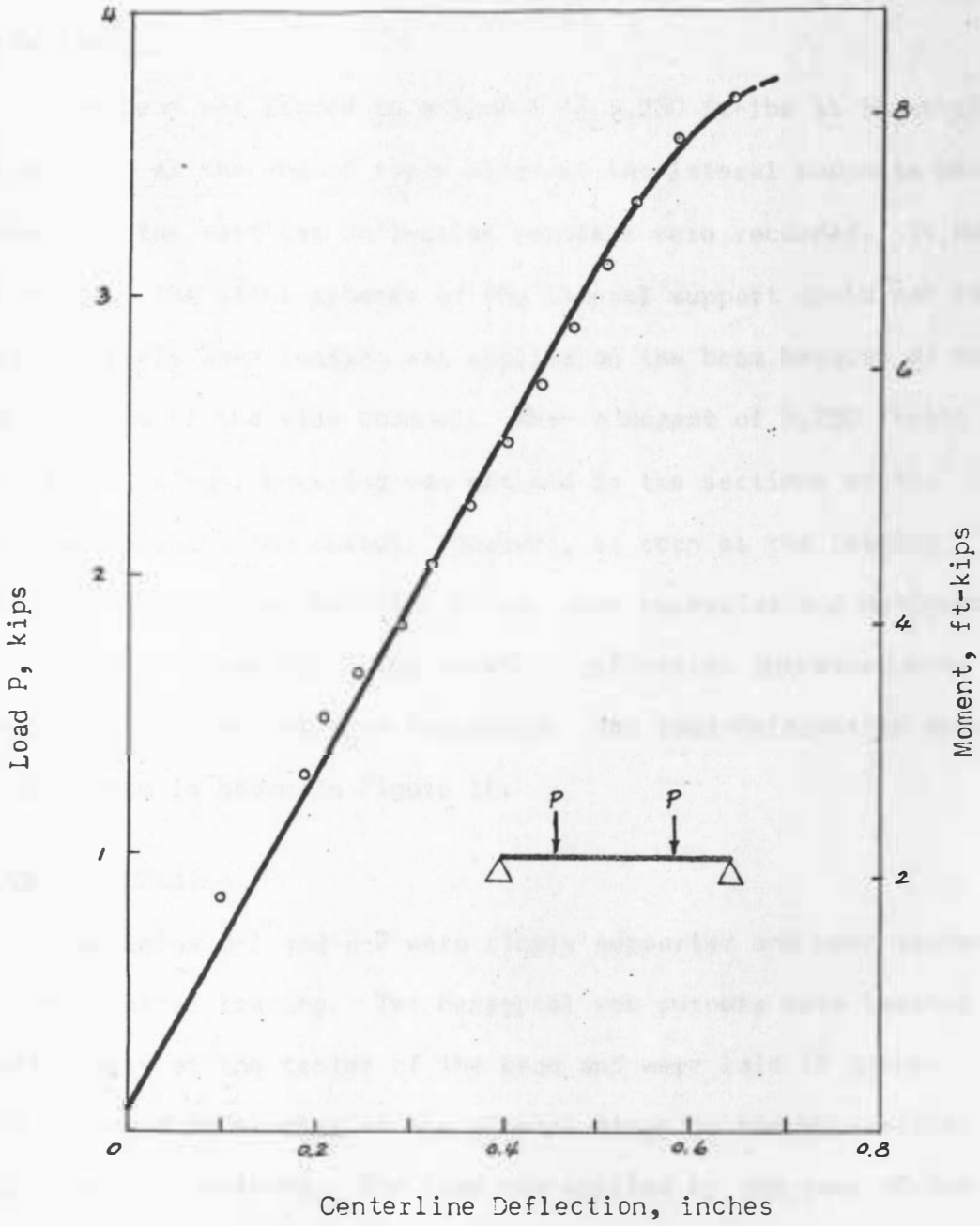

Figure 17. Load Deformation Relationship for Beam A-1

Five lateral supports were placed on the testing specimen as shown in Figure 11. The same test procedure as used in specimen A-1 was followed.

The beam was loaded to a moment of 8,250 ft-lbs at intervals of 218 pounds. At the end of every interval the lateral supports were checked and the vertical deflection readings were recorded. It was noticed that the steel spheres of the lateral support could not roll or slide freely when loading was applied on the beam because of the rough surface of the side channel. When a moment of 8,250 ft-lbs was reached, slight buckling was noticed in the sections of the upper flange above the cutout. However, as soon as the loading increased, the lateral buckling became very excessive and noticeable, and it increased rapidly. The vertical deflection increased even though the load had not been increased. The load-deformation behavior for this beam is shown in Figure 18.

B. Center Loading

Specimens B-1 and B-2 were simply supported and were tested with one central loading. Two hexagonal web cutouts were located symmetrically at the center of the beam and were laid 10 inches apart to avoid developing of any plastic hinge in the web-section upright between cutouts. The load was applied by the same 60-ton hydraulic jack, pulling the assembly downward. A dial gage was mounted at the center of the beam to measure the vertical deflection.

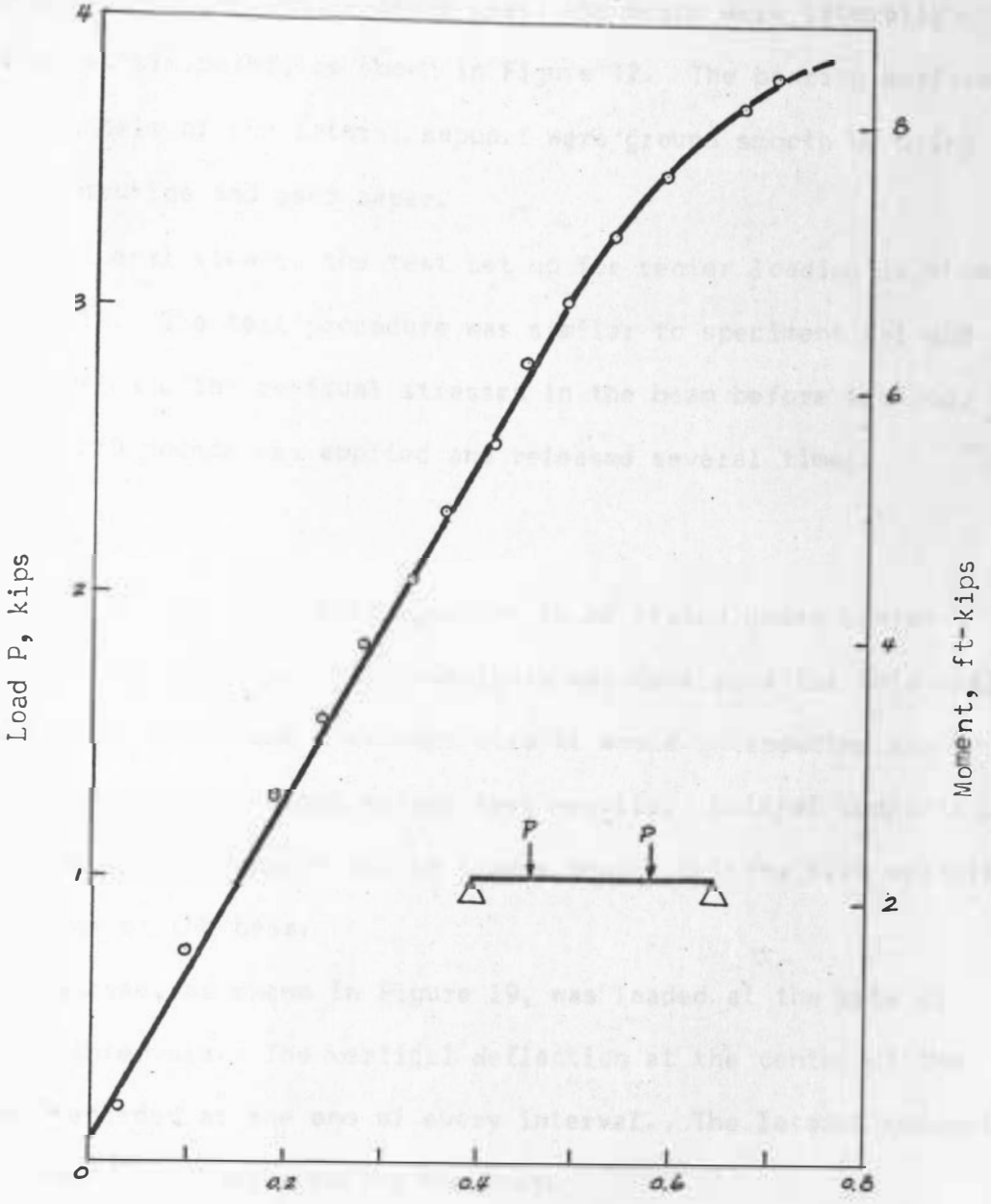

Figure 18. Load Deformation Relationship for Beam A-2

To assure that instability of the beams would not occur prior to the attainment of the ultimate load, the beams were laterally supported at six points as shown in Figure 12. The bearing surfaces of the channels of the lateral support were ground smooth by using a milling machine and sand paper.

A general view of the test set up for center loading is shown in Figure 12. The test procedure was similar to specimens A-1 and A-2. To release the residual stresses in the beam before testing, a load of 550 pounds was applied and released several times.

Specimen B-1

Beam B-1 was the first specimen to be tested under center loading. Since the theoretical analysis was developed for this case, the test was carried out with much care to avoid introducing any other variables which might affect test results. Lateral supports were lubricated with heavy oil to insure smooth rolling with vertical deformations of the beam.

The beam, as shown in Figure 19, was loaded at the rate of 218 pound intervals. The vertical deflection at the center of the beam was recorded at the end of every interval. The lateral supports were checked continually during the test.

The beam was loaded to 3,346 pounds. This weight included the beam and the weight of the assembly hanging on the beam. Initial yielding occurred at the upper right corner of the right cutout as well as the equivalent position of the left cutout. This was indicated by the flaking of the white wash at these two locations as shown in

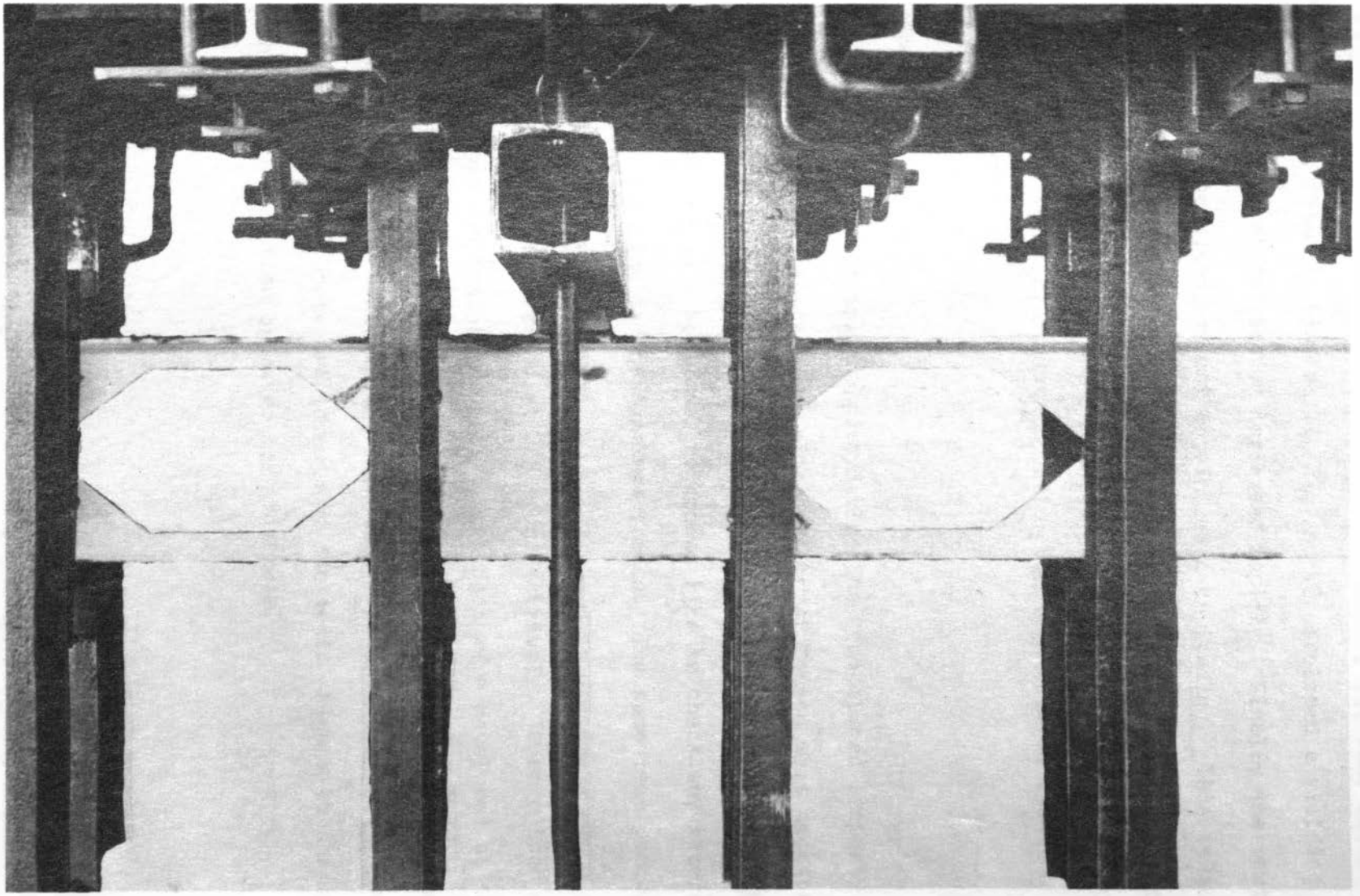

Figure 19. Back View of Specimen B-1 Before Testing

Figure 20. When the load exceeded 3,346 pounds, all four corner portions as shown in Figures 21, 22, and 23 developed a yielding zone and vertical deflection increased rapidly. Finally the vertical deflection increased without any increase in loading. This indicated that a sufficient number of fully-plastic hinges had formed and the beam had failed. The highest load recorded for the test was 3,564 pounds. The load deformation behavior for this beam is shown in Figure 24.

Specimen B-2

Since the lateral support devices had functioned properly throughout the first test, no alternations of design were necessary. However, a nylon wire was tightened and was set parallel to the beam. The wire served as a horizonal reference line to check any lateral deflection occuring as the beam was loaded. The same test procedure to specimen B-1 was followed.

The beam was loaded at 218 pound intervals. When a load of 3,564 pounds was reached four plastic hinges were developed at the portions of the flange around the four corners of the cutouts, and the beam collapsed exactly as happened to specimen B-1. No lateral deformations were detected throughout the test. Figure 25 shows the load-deformation behavior for this beam.

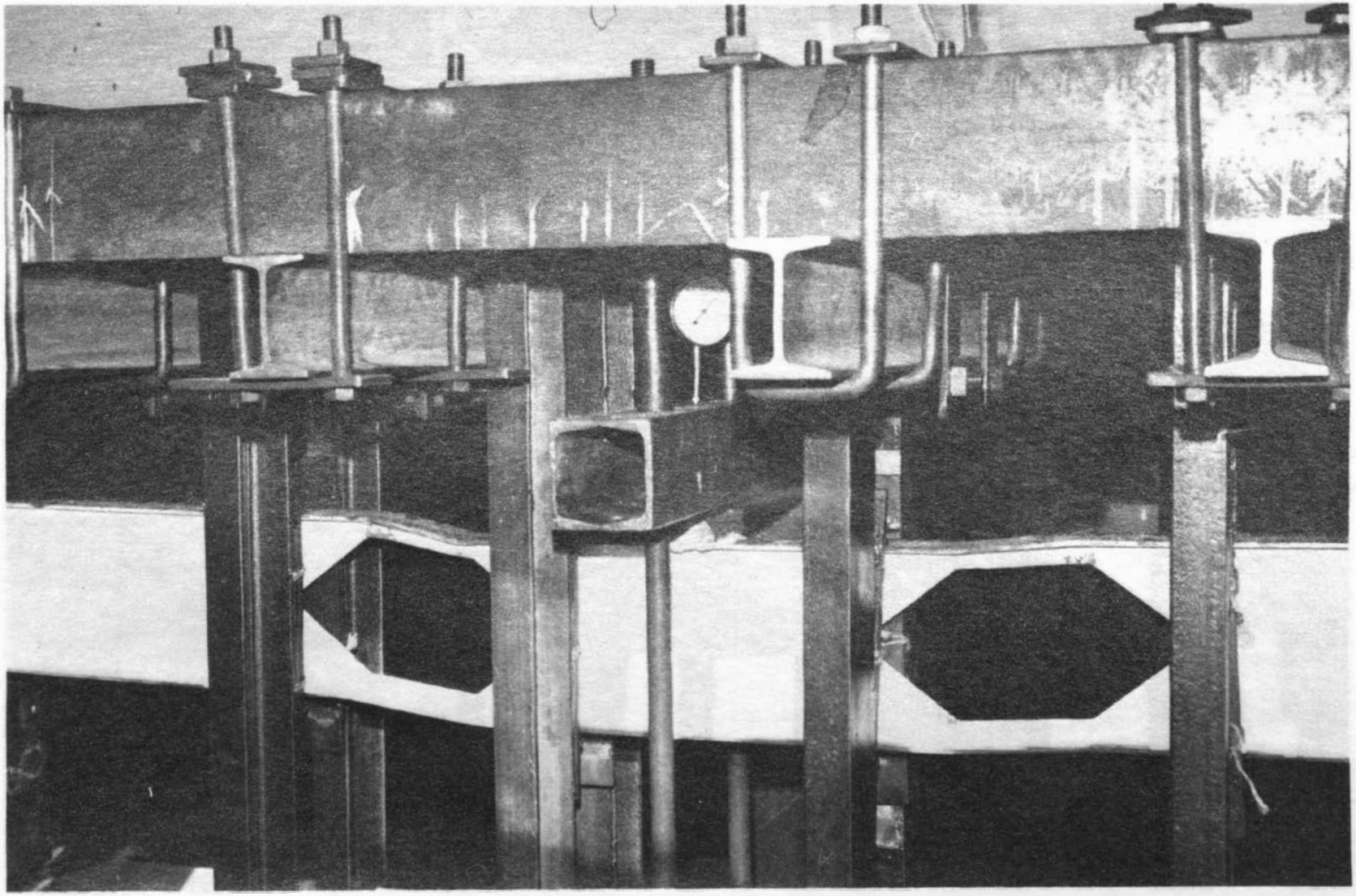

Figure 20. View Showing Initial Yielding Occurred to Specimen B-1

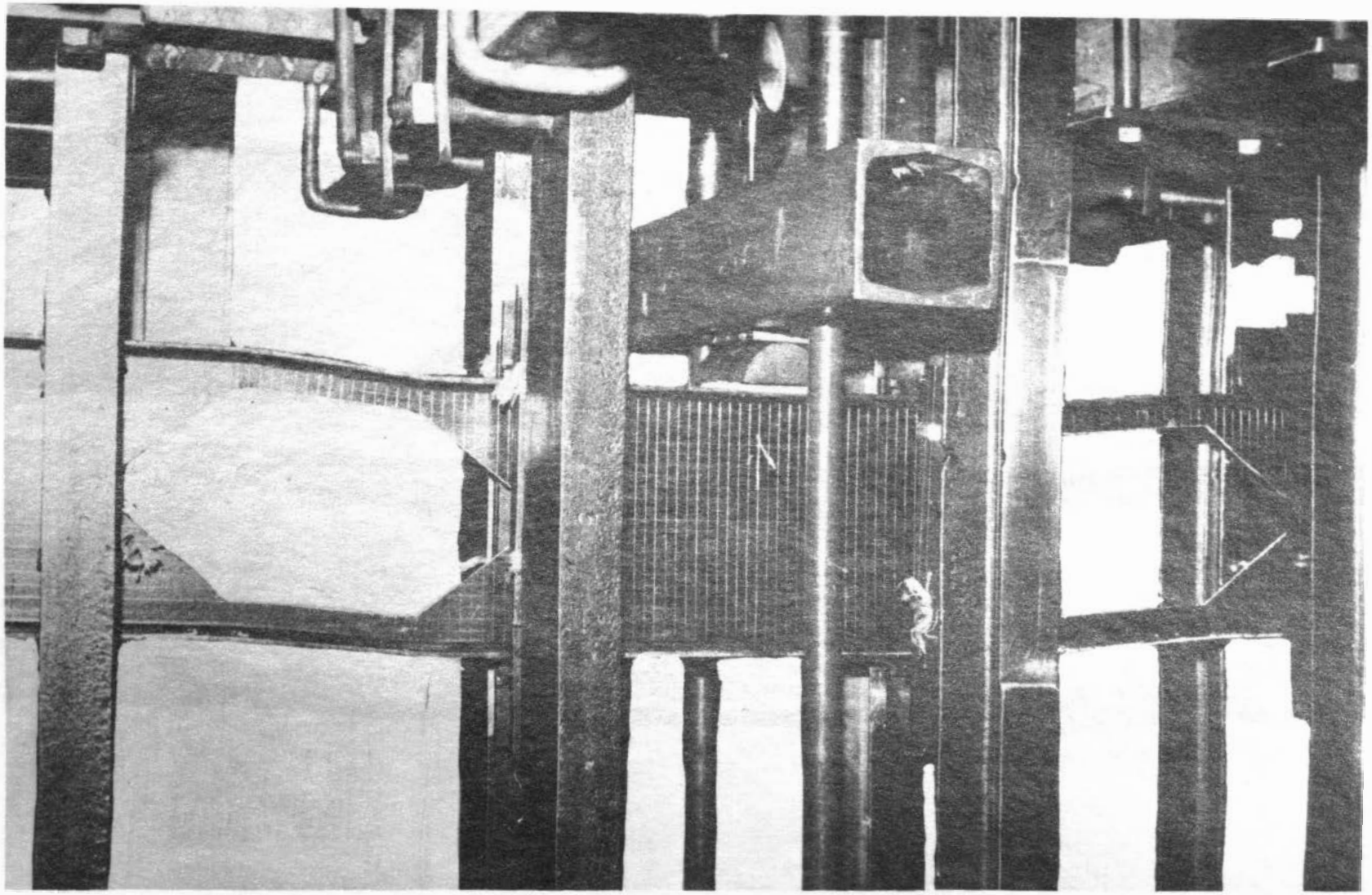

Figure 21. Specimen B-1 During Testing

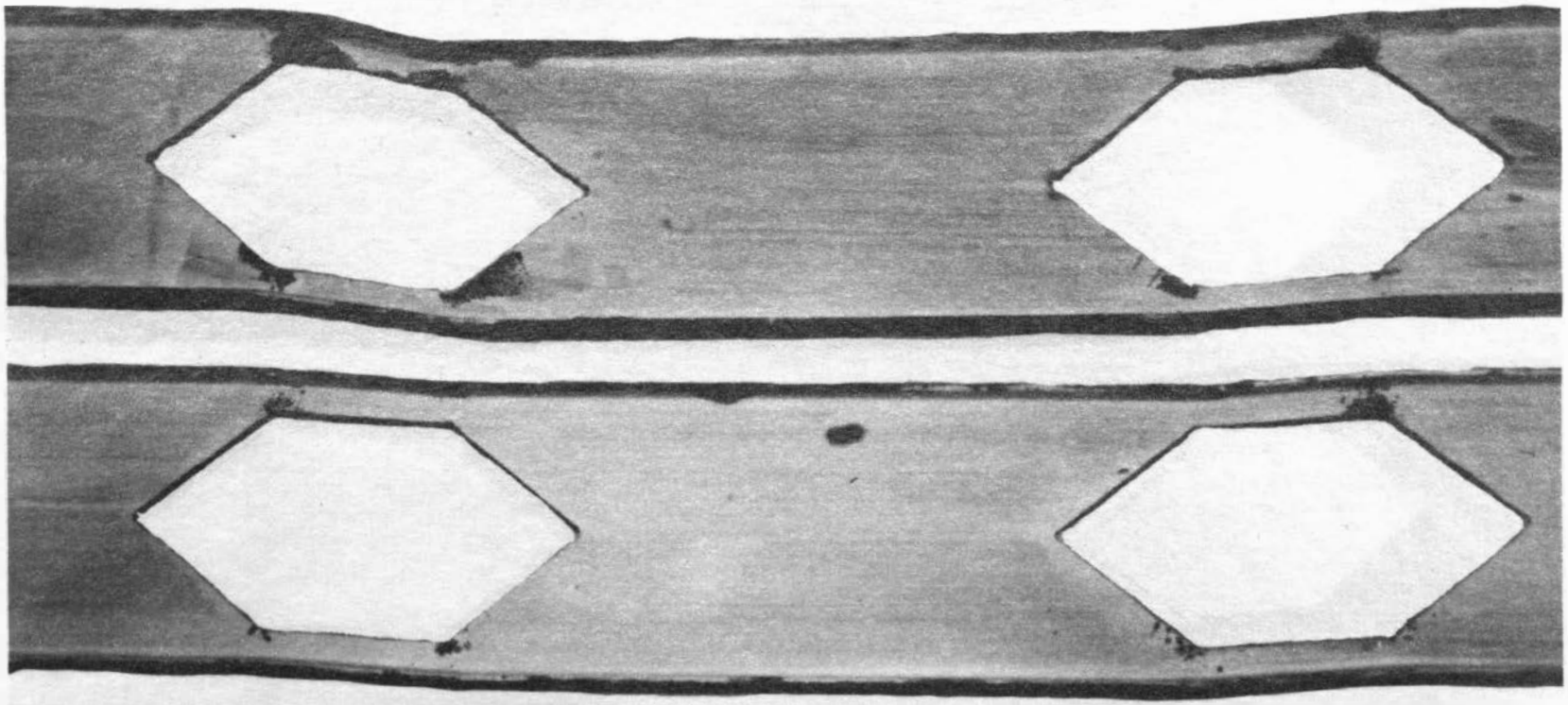

Figure 22. Back View of Specimens B-1 and B-2 Showing Yielding Zones

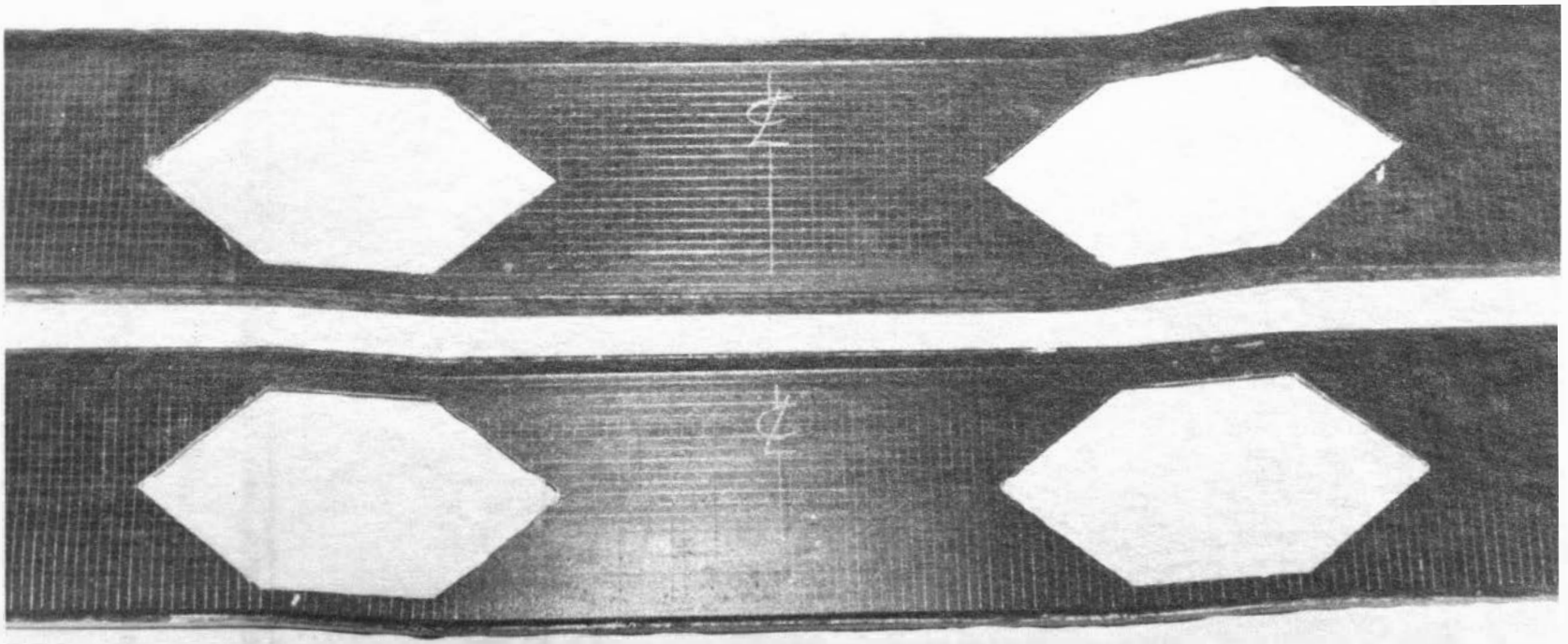

Figure 23. Front View of Specimens B-1 and B-2 After Testing

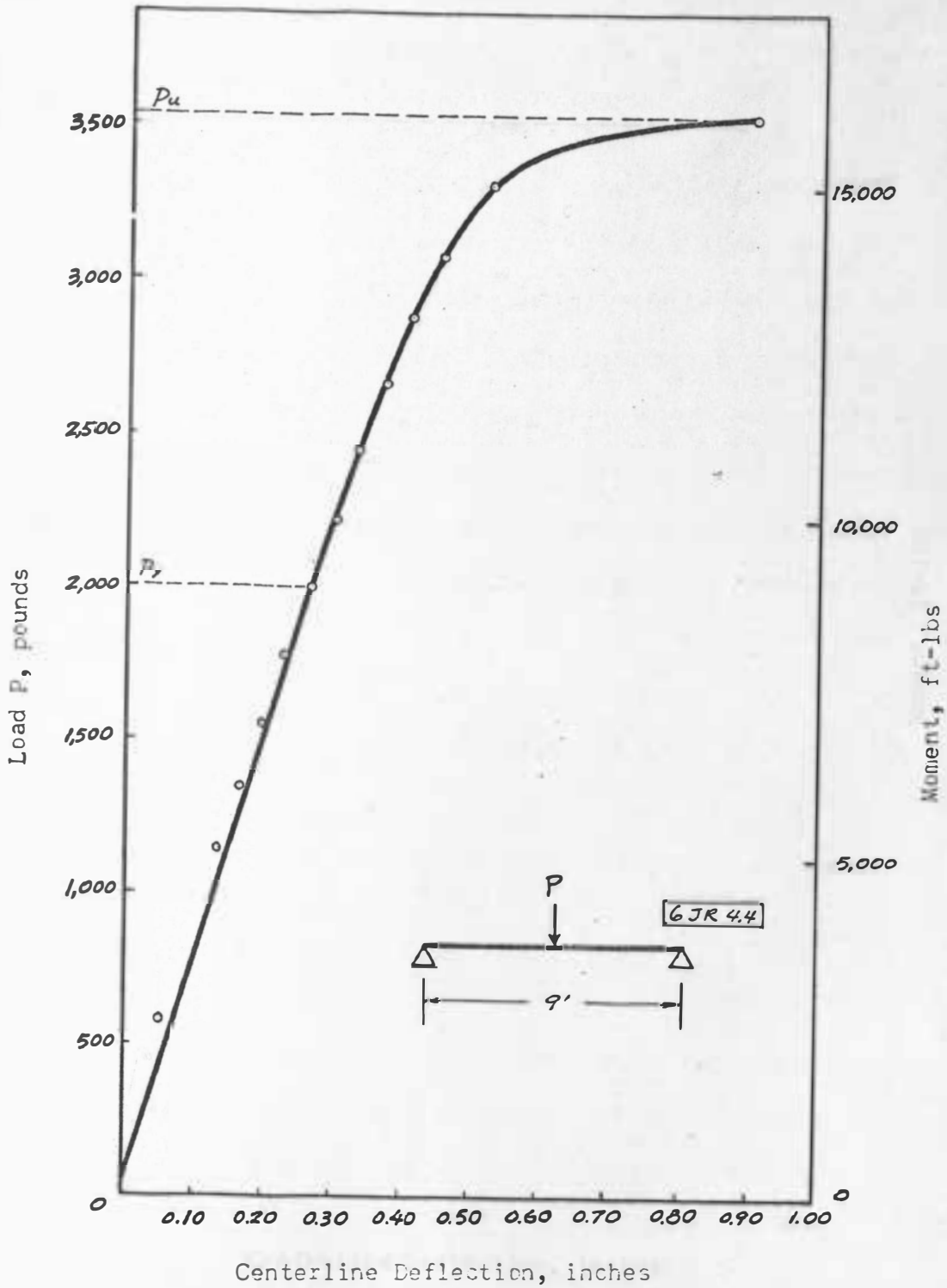

Figure 24. Load Deformation Relationship for Beam B-1

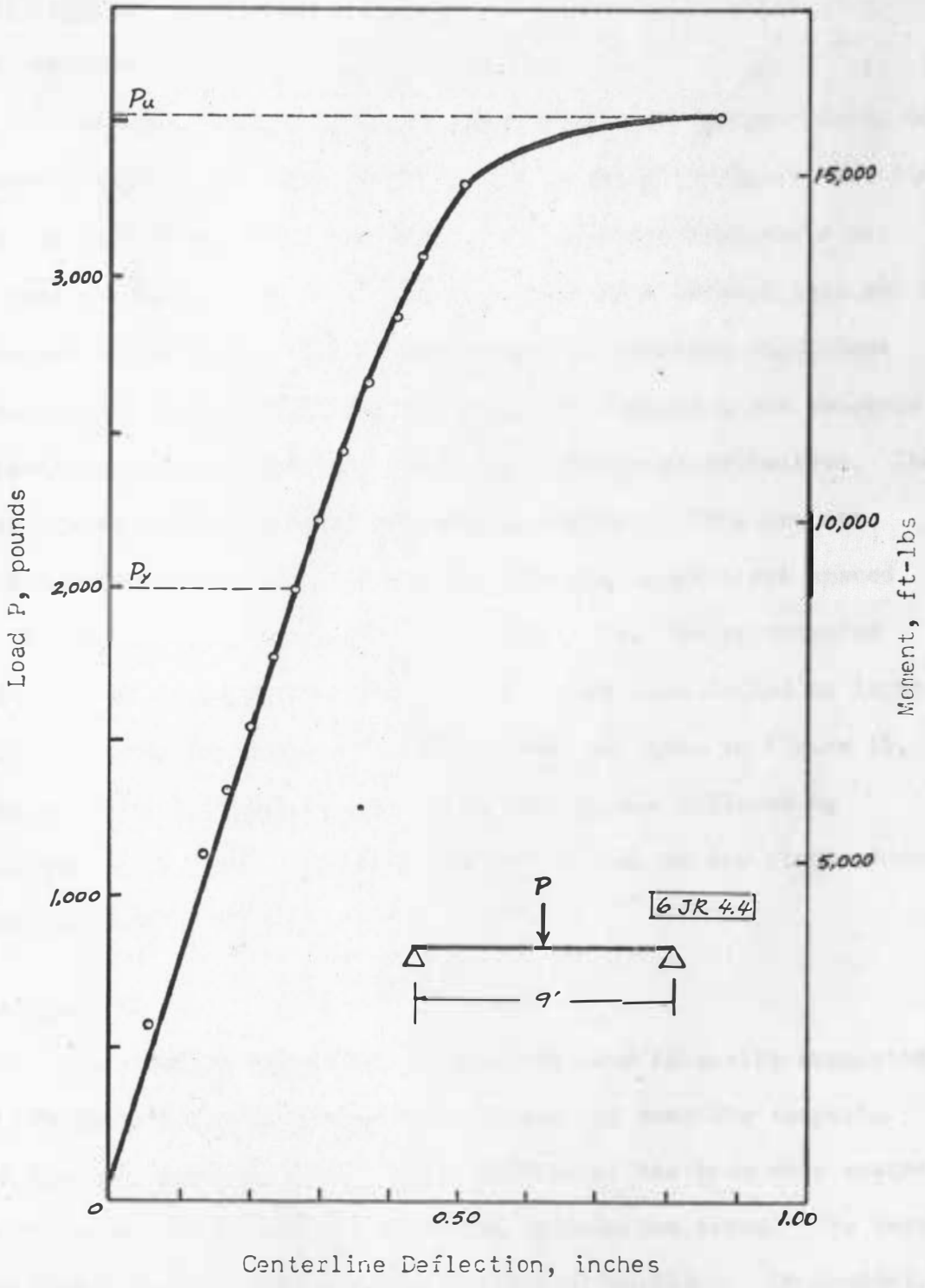

Figure 25. Load Deformation Relationship for Beam B-2

Test Results

Specimen A-1

The beam retained a linear load-deflection characteristic to approximately 90 % of the ultimate load as shown in Figure 17. Since the maximum deflection of the beam under ultimate load could not be predicted directly, no comparison can be made between this and the observed deflections. The lateral supports, however, might have contributed some restraint to the beam, and therefore the observed deflection may have been less than the theoretical deflection. The beam failed due to insufficient lateral support. This was not surprising since the lateral bracing near the support was spaced at 40 inches. This spacing is much larger than the recommended values given by Equations (21) and (22). The beam failed by lateral buckling under the upper left loading pad, as shown in Figure 15, with a moment of 8,062 ft-lbs. This failure was followed by buckling of the upper flange in the region just to the right of the buckling failure zone.

Specimen A-2

As shown in Figure 11, five points were laterally supported in addition to the clamp type lateral bracing over the supports. The lateral supports in the center portion of the beam were spaced at 14 inches which was just about the recommended value. The beam was loaded and eventually failed by lateral buckling. On inquiry, it was realized that r_y in equations (21) and (22) should have been modified because of the existence of the cutouts. Actually, the

most critical situation with respect to lateral buckling exists when the beam is under uniform moment. Lateral bracing must be provided at or in the vicinity of plastic hinges so that plastic moment M_p can be maintained until straining has progressed to strain hardening and failure takes place due to local buckling.

The beam exhibited linear load-deflection characteristic to approximately 75% of the maximum load. The maximum vertical deflection recorded was 0.06 inches larger than specimen A-1 and a moment of 8,250 ft-lbs was reached before the beam failed.

Specimens B-1 and B-2

Specimens B-1 and B-2 were tested under center loading. In figures 22 and 23, it may be seen that the failure mechanism developed with the fully-plastic hinges formed in the flange. This failure mechanism was exactly as expected since the fully-plastic strength of the web section between cutouts was designed to exceed the fully plastic strength of the flanges.

The geometry of this type of failure mechanism is similar to that of a Vierendeel truss. The panels deformed as parallelograms so that the end section of the beam remained essentially vertical during deformation.

The deflected shape in the center portions of the beam as shown in Figures 22 and 23 may be interpreted as follows:

> The center portion of the beam first deformed downward as the beam deflected; then, as flange hinges began to develop, the section of the beam in that region started to relax, and decrease in curvature.

The slope of the load-deformation curve changed very gradually, indicating the progressive development of inelastic hinges. The two specimens had the same value as the ultimate load which was 3,564 pounds.

The final readings of the maximum deflection were 0.901 inch for Beam B-1 and 0.872 inch for Beam B-2. Both were nearly double the value calculated for a solid beam of the same size under a load of 3,564 pounds.

Figure 26. Top View of Specimens A-1, A-2, B-1, and B-2 After Testing

CHAPTER IV

CORRELATION OF COMPUTER RESULTS WITH TEST RESULTS

For the beams under center loading, the ultimate loads from theoretical analysis were predicted on the basis of the development of four fully-plastic flange-section hinges in each half of the beam. A comparison between computer results, using the Upper Bound Theorem to locate plastic hinges due to point loading, with the test results follows:

TABLE IV

Comparison Between Computed and Experimental Test Results

		u_A (inches)	u_B (inches)	u_C (inches)	u_D (inches)	P_u (pounds)
Computer results		2.0	2.0	2.0	2.0	3,547
Test results	B-1	2.5	2.0	1.7	1.9	3,564
	B-2	2.2	2.0	1.7	2.0	3,564

The hinge locations of the test result were measured by a ruler. The hinges were assumed to exist at the points where the curvature was maximum.

The hinge values are in substantially good agreement for both the computer and test results. Comparison between actual ultimate load and predicted ultimate load obtained by the computer for beams B-1 and B-2 shows only +0.5 % deviation.

The ultimate load, 3,547 pounds, obtained by computer for specimens B-1 and B-2, is equivalent to a plastic moment of 7,980 ft-lbs. This value of plastic moment is in close agreement with the value of 8,062 or 8,250 ft-lbs obtained for specimens A-1 and A-2 respectively. However, since specimens A-1 and A-2 have been failed by buckling, the collapse moment should be less than 7,980 ft-lbs. The deviation may be attributed to some restraint from the lateral supports.

CHAPTER V

SUMMARY AND CONCLUSIONS

Summary of Results

It is evident that the Upper Bound Theorem procedure was a quite effectual method in predicting the fully-plastic load-carrying capacity for the beam with hexagonal web cutouts. It will also be noted that fully-plastic hinges may be formed in the web section between the cutouts as well as developed in the upper and lower flange section of the cutouts. In this case, however, the procedure is far more complex. It will be necessary to try some more failure mechanisms for the new geometry involved and determine the mechanism which will lead to the least load.

The theory does not apply where the beam failure results from buckling or tearing of the upright. Therefore if there is any uncertainty as to the mode of failure, it will be mandatory that tests be conducted rather than relying on the Upper Bound Theorem.

The analysis showed that the diamond-shaped cutout is the strongest for the case of central loading conditions, if the same length and height of cutout were used. The diamond-shape or rectangular cutout are limiting cases of the hexagonal-type cut. The analysis also indicated that for 6-inch I-beams the shape of the cutout was a major factor affecting the strength.

Conclusions

From theoretical analysis and results gathered during the testing of the specimens, the following conclusions were drawn:

1. When subjected to center loading, the steel beam with a single, diamond-shaped web cutout in either half of the beam exhibits the highest load-carrying capacity among the other cutout configurations considered. All cutouts mentioned above were of equal length and height. Therefore when there is no restriction to the shape of cutouts, the diamond-shape is certainly the best choice. A rectangular web cutout should be avoided.
2. The ultimate load-carrying capacity of the steel I-beam with hexagonal web cutouts can be predicted by using the Upper Bound Theorem and the mechanism method of analysis, if buckling or tearing would not cause failure before the fully-plastic load can be developed.
3. Lateral buckling becomes more important when a beam with hexagonal cutouts is used because of the reduction in cross section. As happened in the first two tests, the mode of failure for both beams was by lateral buckling of the compression flange.

Future Areas of Study and Research

1. The analytical and experimental work on multiple hexagonal web cutouts in either half of the I-beam should be undertaken.
2. The use of Lower Bound Theorem in establishing inelastic failure load should be investigated.
3. The optimum design of the cutouts in I-beams should have a more complete investigation.

BIBLIOGRAPHY

1. Beedle, L. S., Plastic Design of Steel Frames, John Wiley and Sons, Inc., New York, 1958, p. 58.

2. Altfillisch, M. D., B. K. Cooke, and A. A. Toprac, "An Investigation of Welded Open-Web Expanded Beams," Welding Research, (Supplement to Welding Journal), Vol. 22, No. 2, February 1957, pp. 77s - 88s.

3. Worley, W. J., "Inelastic Behavior of Alluminum Alloy I-Beams with Web Cutouts," University of Illinois Engineering Experiment Station Bulletin No. 448, 1958.

4. Shanley, F. R., Strength of Materials, McGraw-Hill Book Company, Inc., New York, 1957, p. 30.

5. Beedle, L. S., and Associates, "Plastic Design of Multi-Story Frames," Fritz Engineering Laboratory, Report No. 273.20, Lehigh University, Summer 1965, p. 3.21.

APPENDIX 1

UPPER BOUND THEOREM

According to L. S. Beedle,[7] the Upper Bound Theorem is stated as follows:

> A load computed on the basis of an assumed mechanism will always be greater than or at best equal to the true ultimate load.

If a problem is approached from the point of view of assuming a mechanism, an upper bound to the correct load will be obtained. But this could violate the plastic moment condition.

To find the mechanism such that the plastic moment condition will not be violated, Mechanism Method is used. The procedure for the Mechanism Method is described as follows:

1. Determine number and location of possible plastic hinges.
2. Select possible independent and composite mechanisms.
3. Solve virtual work equations for the lowest load.
4. Carry out moment check to see that the plastic moment value is nowhere exceeded.

---

[7]Beedle, Plastic Design of Steel Frames, p. 58.

APPENDIX 2

COMPUTER PROGRAM

```
    1 FORMAT(35HPROGRAM FOR LOCATING PLASTIC HINGES/)
      PUNCH 1
    3 FORMAT(4X,2HUA,5X,2HUB,5X,2HUC,5X,2HUD,6X,1HP,6X,2HTB/)
      PUNCH 3
    4 FORMAT(4F7.2,F9.3,F8.4)
    5 READ 4, A,B,C,D
      UD=-1.
    9 DO 63 L=1,4
      UD=UD+1.5
      IF (UD-A) 12,12,13
   12 VD=C
      GO TO 101
   13 IF(UD-A-B) 14,14,101
   14 VD=-C*(UD-A-B)/B
  101 UC=-1.
   15 DO 63 K=1,4
      UC=UC+1.5
      IF(UC-A) 18,18,19
   18 VC=C
      GO TO 102
   19 IF(UC-A-B) 20,20,102
   20 VC=-C*(UC-A-B)/B
  102 UB=-1.
   21 DO 63 J=1,4
      UB=UB+1.5
      IF(UB-A) 24,24,25
   24 VB=C
      GO TO 103
   25 IF(UB-A-B) 26,26,103
   26 VB=-C*(UB-A-B)/B
  103 UA=-1.
   27 DO 63 I=1,4
      UA=UA+1.5
      IF(UA-UD) 63,28,28
C     CONTINUE ON NEXT PAGE
```

```
C     CONTINUE FROM PRECEDING PAGE
   28 IF(UB-UC) 63,29,29
   29 IF(UA-A) 30,30,31
   30 VA=C
      GO TO 33
   31 IF(UA-A-B) 32,32,33
   32 VA=-C*(UA-A-B)/B
   33 YA=0.17294-0.0309*VA
      YB=0.17294-0.0309*VB
      YC=0.17294-0.0309*VC
      YD=0.17294-0.0309*VD
      RA=YA/2.+(0.4559-0.3124*VA+0.0544*VA*VA)/(0.3191-0.057*VA)
      RB=YB/2.+(0.4559-0.3124*VB+0.0544*VB*VB)/(0.3191-0.057*VB)
      RC=YC/2.+(0.4559-0.3124*VC+0.0544*VC*VC)/(0.3191-0.057*VC)
      RD=YD/2.+(0.4559-0.3124*VD+0.0544*VD*VD)/(0.3191-0.057*VD)
      XA=(UA+UB)*(UA+UB)
      XB=(UB-UC)*(UB-UC)+(6.-YB-YC)*(6.-YB-YC)
      XC=(UC+UD)*(UC+UD)
      XD=(UA-UD)*(UA-UD)+(6.-YA-YD)*(6.-YA-YD)
      Z=0.1
      Q=1.5708-Z-ATANF((UA-UD)/(6.-YA-YD))
      SA=XA+XD-2.*(UA+UB)*SQRTF(XD)*COSF(Q)
      E=ATANF((SA+XD-XA)/SQRTF(ABSF(4.*XD*SA-(SA+XD-XA)*(SA+XD-XA))))
      H=ATANF((SQRTF(ABSF(4.*XC*SA-(SA+XC-XB)*(SA+XC-XB))))/(SA+XC-XB))
      G=1.5708-E+H
      SB=XC+XD-2.*(UC+UD)*SQRTF(XD)*COSF(G)
      WA=ATANF((UB-UC)/SQRTF(ABSF(XB-(UB-UC)*(UB-UC))))
      WB=ATANF((XA+XB-SB)/SQRTF(ABSF(4.*XA*XB-(XA+XB-SB)*(XA+XB-SB))))
      WC=ATANF((XB+XC-SA)/SQRTF(ABSF(4.*XB*XC-(XB+XC-SA)*(XB+XC-SA))))
      TB=WA-WB
      TC=ABSF(WA+WC)
      TD=ABSF(3.1416-G-Q-Z)
      HA=0.3813+0.114*(C-VA)
C     CONTINUE ON NEXT PAGE
```

```
C     CONTINUE FROM PRECEDING PAGE
      HB=0.3813+0.114*(C-VB)
      HC=0.3813+0.114*(C-VC)
      HD=0.3813+0.114*(C-VD)
      SUM=Z*HA*RA+(ABSF(TB))*HB*RB+TC*HC*RC+TD*HD*RD
      P=SUM*36./((UA+UB)*Z+(A+B+D-UB)*(Z-TB))
      PUNCH 4, UA,UB,UC,UD,P,TB
   63 CONTINUE
      GO TO 5
      END
```

APPENDIX 3

PUMP READINGS, ACTUAL LOAD, AND ACTUAL MOMENT RELATIONSHIP

Pump Readings, Actual Load, and Actual Moment Relationship

Dial Reading (psi)	Beams A-1 and A-2		Beams B-1 and B-2	
	Load (pounds)	Moment (ft-lbs)	Load (pounds)	Moment (ft-lbs)
0	210	455	74	167
50	485	1,050	620	1,395
100	755	1,635	1,165	2,625
120	865	1,875	1,385	3,120
140	1,022	2,220	1,600	3,600
160	1,080	2,340	1,820	4,100
180	1,190	2,580	2,035	4,580
200	1,300	2,820	2,255	5,070
220	1,410	3,050	2,475	5,570
240	1,520	3,195	2,695	6,070
260	1,630	3,530	2,915	6,560
280	1,740	3,770	3,110	7,000
300	1,845	4,000	3,345	7,530
320	1,955	4,325	3,564	8,025

Dial Reading	Beams A-1 and A-2	
	Load	Moment
(psi)	(pounds)	(ft-lbs)
340	2,065	4,480
360	2,170	4,700
380	2,280	4,940
400	2,390	5,180
420	2,500	5,420
440	2,610	5,660
460	2,720	5,900
480	2,830	6,140
500	2,935	6,360
520	3,045	6,600
540	3,155	6,840
560	3,260	7,070

NOTATION

The following notation is used in this thesis:

A = area of cross section

A_t = area of the section where the plastic hinge occurs

a = half the length of the uniformed tee-section

b = length of the tapered tee-section

c = half the depth of cutout

D = distance from support to the near end corner of cutout

d, h = depth of beam

E = modulus of elasticity

L_1, L_2, L_3, L_4 = distance between plastic hinges

L_{cr} = critical length or spacing of lateral supports

M = moment

M_p = plastic moment

P = applied load

P_y = load at which yielding occurs

P_u = ultimate load

r_y = radius of gyratism with respect to the Y-Y axis

S_1, S_2 = diagonal distance between plastic hinges

U = energy

u, v = rectangular coordinates with its origin at the center of cutout

W_E = external work done

W_I = internal virtual work

y = distance from the outer fiber of the flange to the fully plastic neutral surface

$\bar{y}_i$, $\bar{y}_o$ = distance from neutral axis to centroid of half-area

$\delta, \omega, \psi, \gamma$ = angles in between plastic hinges

ϵ = strain

ϵ_y = strain at yield point

θ = angle of rotation

σ = stress at distance y from neutral axis

σ_y = yield stress level

ϕ = angle change